

REPORT ON THE THEME 03-5-1130-2017/2021
SYNTHESIS AND PROPERTIES OF NUCLEI AT STABILITY LIMITS

Leader: M.G. Itkis
Scientific Leader: Yu.Ts. Oganessian

In compliance with the recommendations and decisions of PAC, Scientific Council of JINR, and CP, the primary objectives under the theme 03-5-1130-2017/2021 are the following:

- Synthesis of isotopes of superheavy elements and study of their nuclear properties ;
- Investigation of multi-nucleon transfer processes in collisions of massive nuclei; synthesis of new neutron-rich heavy nuclei;
- Nuclear structure of elements of the "second hundred" (α -, β -, and γ -spectroscopy of the isotopes of transfermium elements);
- Study of the mechanisms of reactions with stable and radioactive nuclei; search for new types of decay;
- Development of research on the chemical properties of SHE;
- Update of the network knowledge base on low-energy nuclear physics.

This document summarizes the results obtained during the whole period of the theme implementation.

SYNTHESIS OF NEW SUPERHEAVY ELEMENTS

In 2017 we continued the experiments that have been started at the end of 2016; these were aimed at synthesis and study of radioactive properties of the neutron-deficient isotopes of flerovium (element 114) and their α -decay descendants produced in the complete-fusion reactions $^{240}\text{Pu}+^{48}\text{Ca}$ at the ^{48}Ca energy of 250 MeV [1]. The total accumulated dose of ^{48}Ca ions was 1.4×10^{19} . The experiments were carried out using the gas-filled separator DGFRS at FLNR JINR in collaboration with the research centers of Oak Ridge (ORNL), Knoxville (UT), Warsaw (UW), Nashville (VU), Olomouc (PU), Livermore (LLNL), and Lanzhou (IMP).

Three decay chains of the isotope ^{285}Fl including five its decay daughters from ^{281}Cn to ^{265}Rf have been produced (Fig. 1). Radioactive properties of most nuclei in the chains agree well with the data obtained from observing a single chain detected in experiment with the BGS separator (Berkeley, USA) in the reaction $^{242}\text{Pu}(^{48}\text{Ca},5n)^{285}\text{Fl}$ and the three chains we produced earlier in the reaction $^{240}\text{Pu}(^{48}\text{Ca},3n)^{285}\text{Fl}$ using DGFRS. However, in the last chain presented in Fig. 1, the decay time of ^{269}Sg exceeded by a factor of 33 the average lifetime derived from the

correspond to the expected maximum cross sections of the 2n- and 3n-reaction channels. We have detected 55 new decay chains of ^{288}Mc and 6 of ^{289}Mc . Due to the higher transmission of the new separator, the number of observed decay chains is almost twice the number of nuclei synthesized in previous experiments performed at DGFRS-1 in 2003-2012. Two typical decay chains of ^{288}Mc and ^{289}Mc are shown in Fig. 2.

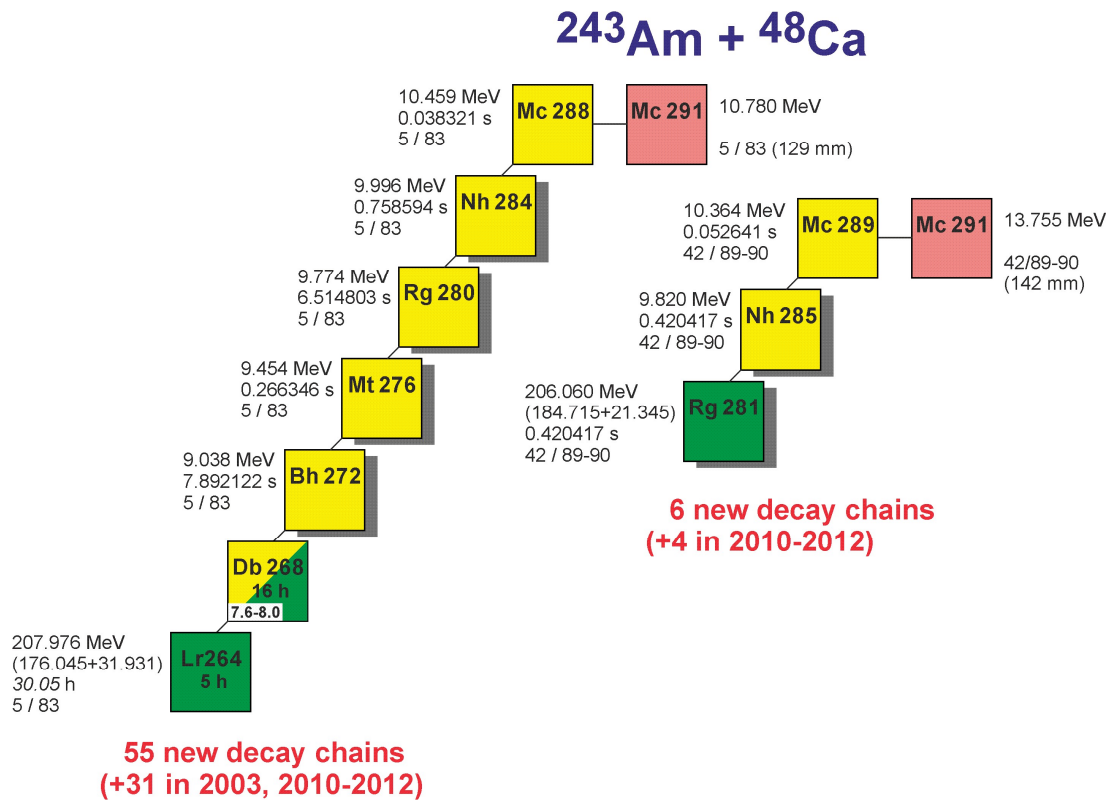


Fig. 2. Decay chains of ^{288}Mc and ^{289}Mc detected in 2020-2021 in the $^{243}\text{Am} + ^{48}\text{Ca}$ reaction.

In present experiments, we attempted to register α decay of ^{268}Db . The preliminary results of the data analysis are shown in Fig. 3. Owing to the higher suppression of the background reaction products in the new separator, we were able to observe for the first time the α decay of ^{268}Db , measure α -particle branch for ^{268}Db which may exceed $61 \pm 13\%$, and register a new spontaneously fissioning isotope ^{264}Lr with half-life of 5 h (Fig. 2). Note that all the previous estimates of the ^{268}Db half-life were derived from the time distribution between ^{272}Bh and fission fragments, which should be now related mostly to the isotope ^{264}Lr . Therefore, one can conclude that the ^{268}Db half-life of 16 h is also measured for the first time.

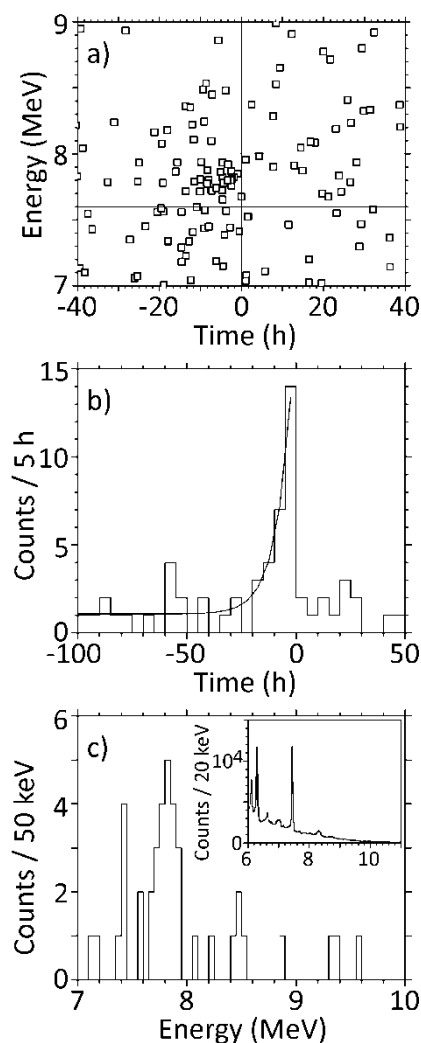


Fig. 3. (a) Energy-time distribution of α -like events preceding and following fission fragments (SF) observed in the decay chains of ^{288}Mc with respect to the registration time of SFs. (b) Time distribution of α -like events with energies $E_{\alpha}=7.6\text{-}8.0$ MeV. (c) Energy distribution of α particles detected within 5 h prior to SFs. Insert demonstrates non-random origin of events with $E_{\alpha}=7.6\text{-}8.0$ MeV.

This $^{243}\text{Am}+^{48}\text{Ca}$ reaction, as well as the reaction $^{242}\text{Pu}(^{48}\text{Ca},3\text{-}4\text{n})^{286,287}\text{Fl}$, will be used to study the chemical properties of the elements Nh, Mc, Cn and Fl. The relevance of these studies is associated with the possibility to compare the properties of these elements with the properties of their homologues. Thus, it is possible to experimentally determine the influence of relativistic effects on the chemical properties of the heaviest elements, to get information concerning the compliance of the chemical behavior of superheavy elements with the law of periodicity of properties, which is extremely important for understanding the structure of the Periodic Table of elements. The DGFRS-2 or DGFRS-3 separators will be used as preseparator in front of the chemical facility. To select the optimum parameters of the separator and the chamber of the chemical facility, it is necessary to measure the distribution of nuclei in the focal plane of the

separator. In the same experiments, the decay properties of the synthesized nuclei will also be studied in more detail.

In March 2021, we have performed the first experiment aimed at the synthesis of Fl ($Z=114$) isotopes in the $^{242}\text{Pu}+^{48}\text{Ca}$ reaction. During about a week, we observed 12 decay chains of $^{286,287}\text{Fl}$. As in the previous case, the yield of nuclei synthesized at DGFRS-2 is almost three times larger than that observed at DGFRS-1 under similar experimental conditions.

New experimental facilities. The first experimental facility, aimed at continuing study of the superheavy nuclei at the Super-Heavy Elements Factory of FLNR, JINR (SHE Factory), is a new gas-filled separator DGFRS-2. The separator was designed in FLNR and manufactured by SIGMAPHI (France). In 2018, installation of the main components of the separator has been completed. The first quadrupole lens Q_1 focuses vertically the nuclei knocked out of the target to increase the efficiency of their transport through the gap of the magnet D_1 , where the products of the complete-fusion reactions (ERs) are separated from the bulk of the beam particles and the products of background reactions. The ERs are then focused by two quadrupole lenses Q_2 and Q_3 . The magnet D_2 is installed for additional separation of ERs from background particles.

Other essential components of DGFRS-2 have been designed and manufactured: these are the system of differential pumping of gas that is to provide gradient of pressure from 1 Torr in the separator to 10^{-7} Torr in the beam line and the target modules. At the end of 2018, the detection system module and the supports for the parts of the beam line have been delivered.

During 2019 the work on commissioning of all the units of the separator DGFRS-2 (Fig. 4) was completed. All the beam line elements are mounted ahead of the separator. Components have been developed and installed for control of the vacuum systems of the beam line and separator, for measuring the parameters of the ion beam, for supplying gas in the separator, for control of the magnetic elements, control and safety components of the vacuum systems.

The first test experiments were carried out in order to determine the optimum parameters of the DGFRS-2 using α particles and products of the reaction $^{\text{nat}}\text{Yb}(^{40}\text{Ar},xn)^{207-212}\text{Ra}$. Experiments were launched with the ^{48}Ca beam and targets of $^{\text{nat}}\text{Yb}$, ^{174}Yb , ^{170}Er .

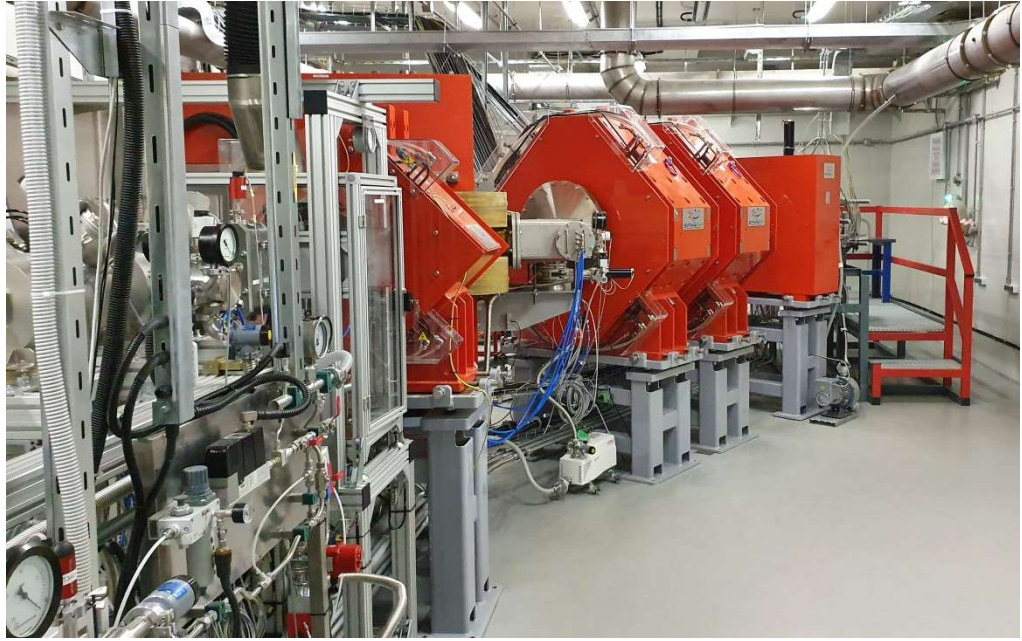


Fig. 4. Photo of the gas-filled separator DGFRS-2.

In 2020, test experiments were continued with an aim to determine the optimum parameters of the DGFRS-2 gas-filled separator for transporting the reaction products of ^{48}Ca with targets of $^{\text{nat}}\text{Yb}$, ^{174}Yb , ^{170}Er , and ^{206}Pb . These tests are required for preparing experiments on synthesis and study of the superheavy nuclei (SHN). This series of experiments have shown that for a more efficient collection of nuclei, it is necessary to increase the detector size in the separator's focal plane. A new system of detectors with a size of $48\text{ mm}\times 220\text{ mm}$ was developed, assembled and tested (Fig. 5). This makes it possible to increase the collection efficiency of reaction products by a factor of 1.5, which is of extreme importance for running long-term experiments on the synthesis of SHN. With these new detectors, we determined the optimum setting of DGFRS-2, the dispersion of dipole magnets, the effect of gas pressure on the separator transmission and on the equilibrium charge of ions – products of the reactions ^{174}Yb , $^{206}\text{Pb}+^{48}\text{Ca}$.

In November 2020, we started an experiment in order to study in detail the properties of Mc isotopes and their production cross sections in the complete-fusion reaction $^{243}\text{Am}+^{48}\text{Ca}$.

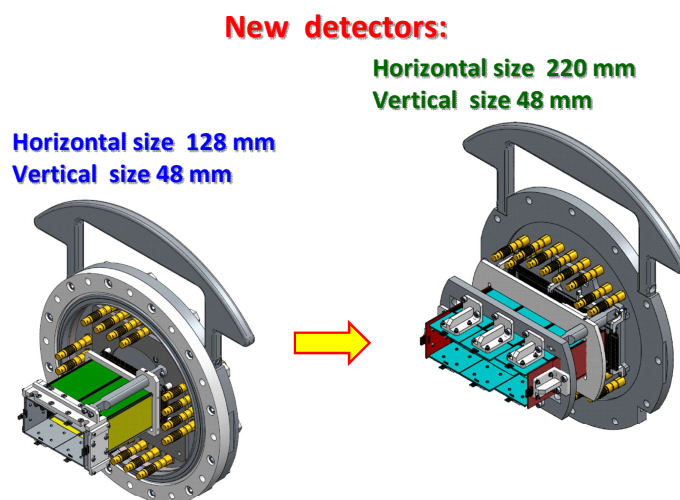


Fig. 5. Schematic image of the initially used and new detector arrays of the separator DGFRS-2.

Main results on the synthesis and study of the properties of SHE are published in [1–11].

SPECTROSCOPY OF HEAVY AND SUPERHEAVY NUCLEI.

In the 2017, spontaneous fission properties of ^{254}Rf formed in the reaction ^{50}Ti on ^{206}Pb target were studied. The intense ^{50}Ti beam was provided by the U400 using the Metal Ions from Volatile Compounds (MIVOC) method. The neutron yield from the spontaneous fission of the short-lived neutron-deficient ^{254}Rf nucleus is measured using the combined detection system of the SHELS velocity filter. The half-life and the branching ratio of ^{254}Rf are also measured. The data on the multiplicity of prompt neutrons from spontaneous fission of ^{254}Rf ($\bar{\nu} = 3.87 \pm 0.34$) are presented for the first time [12]. The available experimental data on the average number of neutrons per fission obtained for spontaneous fission of isotopes from Pu to Db are presented in Fig. 6.

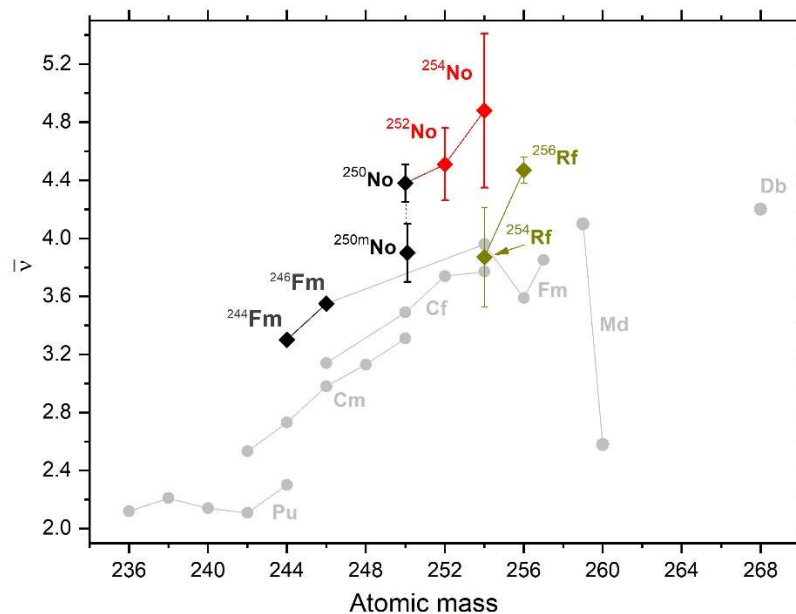


Fig. 6. Average number of neutrons per spontaneous fission (circles) as a function of A . Diamonds are the results obtained at SHELS.

A fission branch of ^{255}Rf has been registered. The half-life obtained from the fission events is 1.69(4) s for ^{255}Rf and 7.3(4) ms for ^{256}Rf (corresponding to 1n evaporation channel). In total 1600 ^{255}Rf fission events are observed and ~ 430 of ^{256}Rf fission events. The number of observed alpha decays and fission events allows to deduce the fission branch of ^{255}Rf to be 44 %.

The half-life of the isomeric state in ^{255}Rf is found to be 59(6) μs . The fact that there are high-energy γ rays means that the excitation energy of the isomer is rather high as in the case of ^{257}Rf .

The $^{50}\text{Ti} + ^{206,208}\text{Pb}$ reaction was used for the study of the radioactive decay properties of the $^{254,256,257}\text{Rf}$ isotopes. Several isomeric states in the isotopes $^{254,256,257}\text{Rf}$ with the half lives ranging from 5 to 200 μsec were detected. Fig. 7 gives the data on the fine structure of the α -decay of the ^{257}Rf mother nucleus to the ^{253}No daughter nucleus. The $11/2^-$ state of the ^{253}No nucleus was for the first time observed, and the $1/2^+$ state (451-KeV level) detected earlier was confirmed.

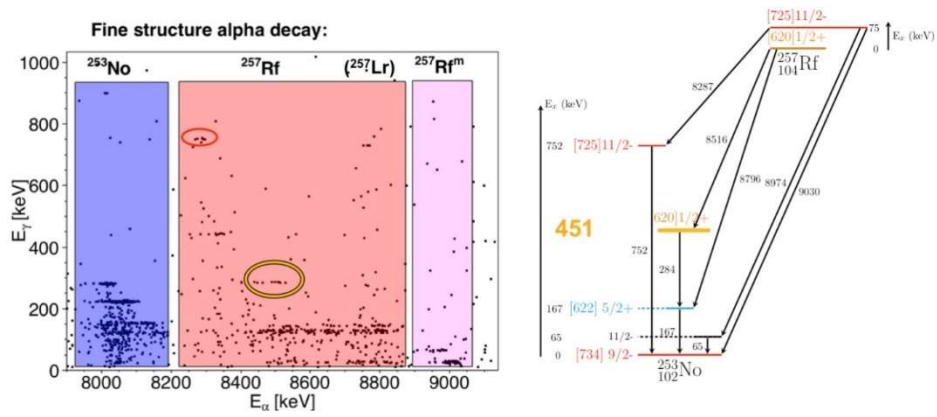


Fig. 7. Fine structure of the α -decay of the ^{257}Rf mother nucleus

The isotopes $^{256,257,258}\text{Db}$ were produced in $^{50}\text{Ti}(^{209}\text{Bi}, \text{xn})^{259-x}\text{Db}$ reactions. The analysis of fission events following the implantation of evaporation residues produced in the fusion reaction of ^{50}Ti and ^{209}Bi at different bombarding energies has revealed 5 millisecond decays, which are attributed to the spontaneous fission of proton-evaporation channels. The average cross sections for proton evaporation are found to be ~ 100 and 10 times smaller than the largest neutron-evaporation channel cross section at the same excitation energy (see Fig.8). These results suggest that the proton evaporation channel, albeit weak, may represent a realistic alternative to synthesize new, more neutron-rich superheavy nuclei [13].

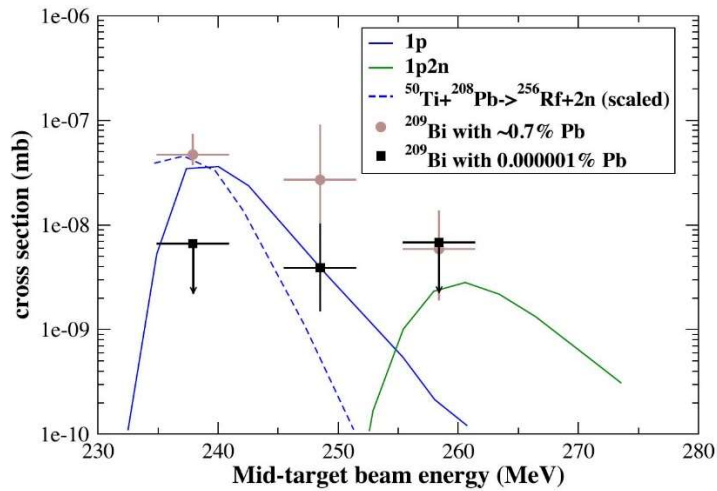


Fig. 8. Experimental and theoretical cross sections for pxn evaporation as a function of mid-target beam energies and target Bi enrichment. The solid lines are the result of theoretical calculations for the p and $p2n$ evaporation channels and the dashed line is the scaled cross section for the $^{50}\text{Ti}(^{208}\text{Pb}, 2n)$ reaction.

$^{254,252,250}\text{No}$ were studied with a ^{48}Ca beam and high purity Pb targets. The aim was to study the electromagnetic and fission branches of the known K isomers in these nuclei. For the ^{250}No case, the electromagnetic branch from the $\sim 40 \mu\text{s}$ isomer has been confirmed. The observation of

gamma-rays and internal conversion electrons has allowed a complete decay scheme to be established, allowing for the determination of the spin, the parity and excitation energy of the isomer. The measured fission branch now represents one of the few firm cases where the fission branch of an identified high-K isomers has been measured [14].

The $^{238}\text{U}(^{22}\text{Ne},\text{xn})^{260-\text{x}}\text{No}$ reaction was used to produce No nuclei. Isomeric states in ^{256}No were investigated using internal conversion electron and γ -ray spectroscopy with the GABRIELA detection system at the focal plane of the SHELS recoil separator. The emission of internal conversion electrons and γ -rays occurring between a ^{256}No implantation and a subsequent alpha decay event were studied, resulting in the observation of high-K isomerism in this nobelium isotope. The nature of the isomeric states are discussed in terms of possible 2-qp and 4-qp structures [15].

In February 2020 experiments aimed at studying the complete fusion reactions of $^{38,40}\text{Ar}$ beams and ^{208}Pb , ^{232}Th targets were carried out at the SHELS separator. The experimental investigation of the $^{40}\text{Ar} + ^{208}\text{Pb} = ^{248-\text{x}}\text{Fm} + \text{xn}$ reaction aimed at measuring the excitation function and specifying the properties of the radioactive decay of the nucleus of ^{246}Fm . The $^{38}\text{Ar} + ^{232}\text{Th}$ reaction was studied under the assumption that the ^{266}Sg nucleus and an α -particle were formed in the exit channel. One event was registered during the ten-day irradiation of the ^{232}Th target with ^{38}Ar ions, which can be attributed to spontaneous fission of ^{262}Rf , the ^{266}Sg α -decay daughter nucleus. Taking into account the efficiency of registration of such events, the yield of ^{266}Sg nuclei in the reaction under investigation was lower by a factor of 10 to 30 compared to that we had expected.

The properties of the radioactive decay of the $^{249,250,251}\text{No}$ isotopes observed in the $^{48}\text{Ca} + ^{204}\text{Pb}$ reaction were studied. In our experiments, we used the integrated detection system GABRIELA (α , β , and γ -spectrometry) [16]. The experimental data is preparing for publication. In studies of the complete fusion reaction $^{48}\text{Ca} + ^{204}\text{Pb} = ^{252-\text{x}}\text{No} + \text{xn}$, the regularities were determined for the formation of the nuclei of $^{249,250,251}\text{No}$. The data on internal conversion coefficients for the $^{250\text{m}}\text{No}$ isomeric state decay were supplemented. The half-life and α -decay energy were determined for ^{249}No synthesized in the $3n$ -channel for the first time (Fig. 9).

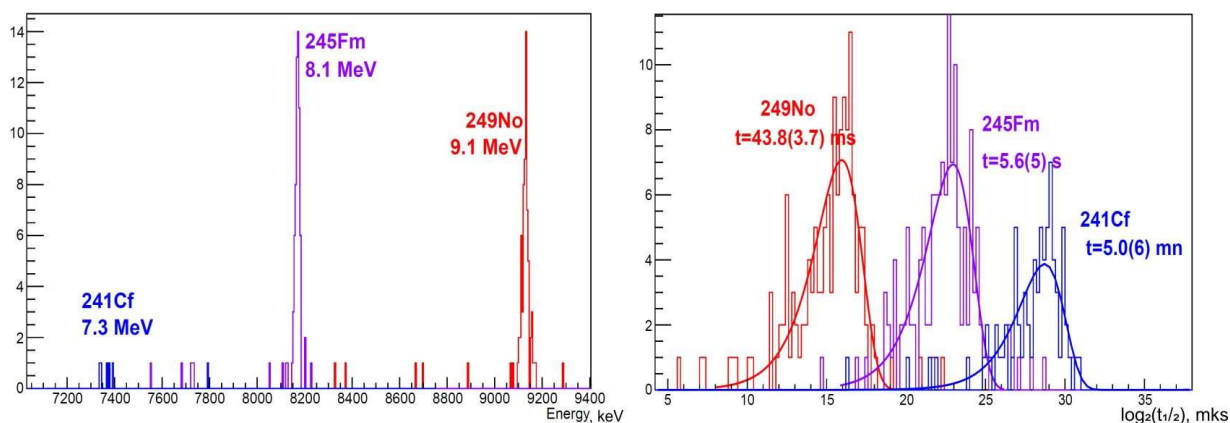


Fig. 9. (left panel) Correlated alpha decays of ^{249}No , its daughter ^{245}Fm and granddaughter ^{241}Cf . (right panel) Corresponding logarithmic decay times with half-lives indicated (preliminary data shown).

CHEMISTRY OF TRANSACTINIDES

In a view of creation of a new experimental complex Factory of Superheavy Elements, research on the chemistry of transactinides in 2017–2021 was focused on the development of a scientific program to study the chemical properties of superheavy elements (SHE) at the new DC-280 accelerator. A unique combination of new facilities and beam characteristics of accelerated heavy ions (the intensity of which is increased by a factor of 5-10) will lead to a significant increase in the efficiency of the experiments. This will make it possible to continue pioneering studies on the study of the chemical properties of 112, 113 and 114 elements, carried out in the previous seven-year period, at a statistically new level. As a result, for the first time, we will be able to answer key questions in this field of research related to the influence of relativistic effects on the law of periodicity of chemical properties for SHE. The main topics of research and developments over the past 5 years include:

- development of an experimental base for chemical research at the SHE factory, including the construction of a setup for conducting research in the gas phase with recoil nuclei on physical separators [17, 18];
- on-line studies on the formation of new compounds of Nh and Fl using their light homologues on the U-400 accelerator under strictly identical conditions by gas thermochromatography [19,20];
- another direction in the study of the properties of Nh is associated with the development of vacuum chromatography and the possibility of using single-crystal synthetic diamonds (CVD) as semiconductor detectors for high-temperature α -spectroscopy in the chemistry of superheavy elements [21];

- development of methods for the manufacture of accelerator targets from enriched isotopes of actinides that are stable under irradiation with high-intensity beams of heavy ions and manufacture of targets from stable and radioactive isotopes of actinides for current experiments;
- development of methods for the synthesis of ^{50}Ti and ^{54}Cr compounds for obtaining ion beams by the MIVOC method and synthesis of metallic ^{48}Ca for obtaining beams of accelerated ions for the synthesis of SHE;
- development of radiochemical methods for the separation of nuclear reactions products and the isolation of radioisotopes from irradiated targets.

Setup has been constructed that combines the capabilities of physical and chemical separation of nuclear reaction products. The advantages of this approach are the separation of the beam and preliminary purification of the synthesized nuclei from the products of nuclear reactions. The main elements of the setup are a gas chamber for collecting separated recoil nuclei installed in the focal plane of a physical separator, a system for fast gas transport of volatile elements or their compounds, and a detector module - a cryodetector, which makes it possible to study the SHE behavior by gas thermochromatography (Fig. 10).

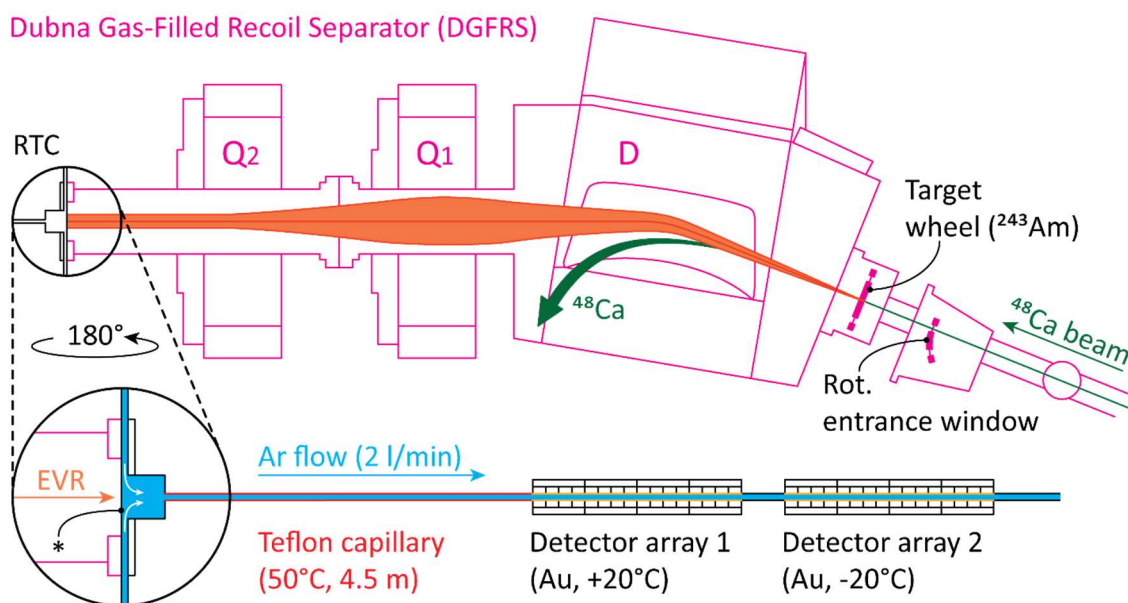


Fig. 10. Schematic representation of the experimental chemistry setup mounted at the DGFRS. The dipole magnet (D) and quadrupole magnets (Q_1 and Q_2) are shown in pink; indicated in orange is the transmission of the evaporation residues (EVRs) through DGFRS and their subsequent transition into the recoil transfer chamber (RTC) through a supporting honeycomb grid and the Mylar foil entrance window (marked by an asterisk). The heated Teflon transport capillary (red), the two detector arrays (bottom right) as well as the gas flow (Ar 6.5, 2 l/min;

shown in blue and with white arrows) are indicated in the bottom part of the figure. The $^{48}\text{Ca}^{18+}$ -ion beam (green) was provided by the U-400 accelerator facility of the Flerov Laboratory of Nuclear Reactions.

A series of such experiments, to study the chemical properties of nihonium in pure conditions, guaranteeing its preservation in elemental form, was completed in 2017 at the DGFRS-1 separator (FLNR) [17]. The experiments included irradiation of ^{243}Am targets with ^{48}Ca beam with an energy of 242 MeV, thermalization of ^{284}Nh ions in a gas chamber, and transport by a gas jet through a Teflon capillary to semiconductor Si detectors with gold surfaces. As a result, the lower limit of the interaction of elemental Nh with the Teflon surface was established $-\Delta H_{\text{ads Teflon (Nh)}} > 45 \text{ kJ/mol}$. We conclude that the transport of Nh isotopes through a Teflon capillary is impossible at room temperature, and that in the thermochromatographic experiments carried out by us earlier, the volatility of Nh was observed not in the atomic state, but in the form of chemical compounds NhO_xH_y .

To study the conditions for the formation of volatile nihonium compounds and prepare for experiments with a higher efficiency at the SHE Factory, research using new setup was continued at the SHELS kinematic separator (FLNR). A new gas chamber for stopping and transport (RTC) recoil nuclei was developed [18]. RTC was mounted at the focal plane of SHELS and separated from the vacuum by a thin mylar foil. A unique feature of this chamber is its speed and the ability to heat up to 650°C , while the separating foil temperature was kept at room temperature, and an isothermal chromatographic column installed immediately behind the chamber with an operating temperature range from room temperature to 900°C (Fig. 11).

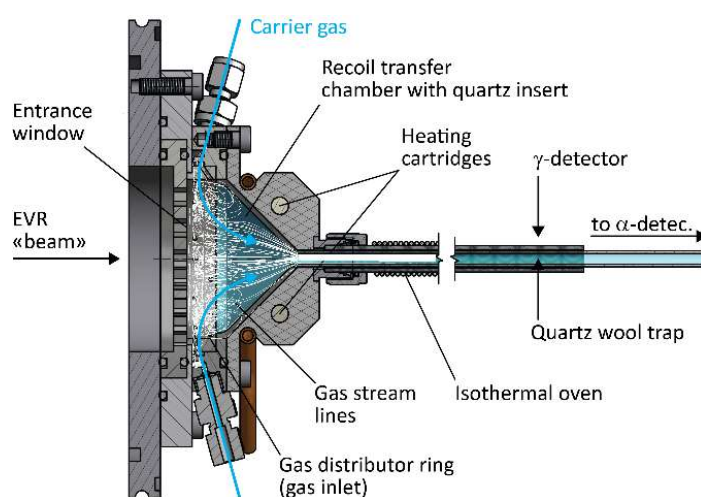


Fig. 11. The experimental setup with the conical recoil transfer chamber and the adjacent isothermal chromatography unit.

This allowed us to study the behavior of thallium, a light homologue of Nh, stopping of recoil nuclei in the gas phase, chemical reactions of hot atoms in pure conditions, kinetics of formation of chemical compounds, yield of chemical reaction products, and their transportation to a chemical detector depending on temperature, water vapor content and composition of gases. The experiments were carried out in on-line mode under conditions strictly identical to those at the SHE factory, producing the short-lived thallium radionuclide ^{184}Tl ($T_{(1/2)} = 10,1 \text{ c}$) in the $^{141}\text{Pr}(^{46}\text{Ti}, 3n)$ nuclear reaction at the U-400 accelerator. The formed volatile thallium compounds were studied by isothermal adsorption chromatography in combination with γ - and α -spectrometry. The results are being analyzed and prepared for publication [19].

Within the framework of cooperation between FLNR and PSI (Switzerland), a series of joint experiments were carried out at the COLD setup to search for new chemical systems for studying Cn and Fl. Analysis of thermodynamic data and preliminary experiments have shown that selenium can be used as a stationary phase in thermochromatographic experiments. The dependences of the enthalpies of formation of selenides of light homologues Cn and Fl are linear and have the opposite sequence in groups. In experiments at the chemical beamline at the U-400 accelerator, FLNR, ^{48}Ca beam and ^{242}Pu target with Nd were used to produce short-lived isotopes of Hg the light homologue of Fl. The limits of the interaction of mercury with the surface of red amorphous and trigonal selenium were determined: $-\Delta H_{\text{ads}}^{\text{red a-Se}}(\text{Hg}) > 85 \text{ kJ/mol}$ и $-\Delta H_{\text{ads}}^{\text{t-Se}}(\text{Hg}) < 60 \text{ kJ/mol}$ [20]. Analysis of the data obtained showed that in thermochromatographic experiments with PIN diodes coating of red amorphous and trigonal selenium using the reaction of ^{48}Ca and ^{244}Pu , it is possible to separate Cn and Fl (produced in the same experiment) and study their properties.

In collaboration with PSI (Switzerland) related to the development of vacuum chromatography, studies of single-crystal synthetic diamonds (CVD) used as semiconductor detectors for high-temperature α -spectroscopy in the chemistry of superheavy elements continued [21]. ^{241}Am was used as a source of α -particles. In this research, the mobility of charge carriers in diamond solid-state detectors was investigated from room temperature to 473 K. In the same temperature range, the α -spectroscopic properties, charge collection, and spectroscopic resolution were analyzed. In all measurements, complete charge collection up to the maximum temperature was observed. The results showed that diamond-based semiconductor solid-state detectors can be used for α -spectroscopy in high-temperature experiments.

STUDY OF HEAVY-ION NUCLEAR REACTIONS AT NEAR BARRIER ENERGIES.

Heavy-ion-induced fusion reactions at bombarding energies around the Coulomb barrier have been very successfully used for the production of superheavy elements (SHE). The main

process hindering fusion towards the synthesis of heavy and superheavy elements is the quasifission (QF) process, a fast process in which the re-separation occurs before the compound nucleus (CN) fully equilibrates. For the better understanding of the QF onset in SHE formed from asymmetric entrance channels, studies on nuclear reactions with medium and heavy nuclei are necessary.

In this framework, in 2017 we have started an experimental campaign at the ALTO facility of IPN Orsay (France) aiming at investigating equilibrium and non-equilibrium processes with the aids of many fold correlations among different probes [22,23]. The goal is to trace the QF process when mixed with the CN-fission events by means of typical observables, such as of mass and total kinetic energy (TKE) of the fission fragments, coupled with the detection of neutrons and γ -rays. These additional probes allow one to scan the distribution of excitation energy and spin along the reaction process.

The features of fragments formed in the near barrier reaction $^{32}\text{S} + ^{197}\text{Au}$ at the beam energy of 166 MeV, leading to the ^{229}Am compound nucleus excited at 43 MeV, were investigated. The time of flight of the binary reaction products were measured by the double-arm time-of-flight spectrometer CORSET. The prompt γ -rays following fission were detected by the ORGAM array and PARIS γ -detection system.

The analysis of the measured neutron and γ -ray multiplicities, total spin distributions confirms the expectation that the main binary decay in the $^{32}\text{S} + ^{197}\text{Au}$ reaction is the CN-fission. This gives us a proof that such a complex multidetector system, along with the complex data analysis tool built, can be reliably used to explore reactions where other reaction processes, such as QF, are known to occur and give rise to binary reactions with larger cross sections than CN-fission process. In those cases, the additional probes, such as γ -rays and neutrons, may allow us to access properties of the reaction not accessible by measuring mass and TKE alone. An extended set of observables measured simultaneously in the same experiment allow one to extract detailed differences with the predictions of the statistical behavior of the formation and decay of binary fragments and to introduce more constraints on models.

To go beyond $Z = 118$ using complete fusion reactions, projectiles heavier than ^{48}Ca must be applied due to the lacking of necessary actinide target materials. However, at the transition to the heavier projectiles, the Coulomb repulsion between the interacting nuclei (Z_1Z_2) increases. The Coulomb factor is one of the key parameters that determine the contributions of QF and deep inelastic processes, which strongly suppress the formation of the CN.

In 2017-2019, to investigate the probability of formation and decay of superheavy systems in dependence on the Coulomb factor Z_1Z_2 at energies around the Coulomb barrier, we conducted a series of experiments aimed at investigating the properties of mass and energy distributions of

binary fragments formed in the reaction of $^{52,54}\text{Cr}$, ^{48}Ti , ^{86}Kr , and ^{68}Zn ions with actinide targets leading to the formation of the superheavy composite systems with $Z = 114$ and 120 [24,25]. A comparative analysis with the results obtained earlier for the reactions with ^{36}S , $^{40,48}\text{Ca}$, $^{48,50}\text{Ti}$, ^{58}Fe , and ^{64}Ni ions allowed us to evaluate fusion probabilities in the wide range of Coulomb factor Z_1Z_2 from 1472 to 2808. The measurements were carried out at the Flerov Laboratory of Nuclear Reactions, Dubna, and the Physics Department of the Jyväskylä University, Finland, using the double-arm time-of-flight spectrometer CORSET. The measured mass-energy distributions of fragments formed in the reactions with heavy ions leading to the formation of composite systems with $Z = 114$ are shown in Fig. 12.

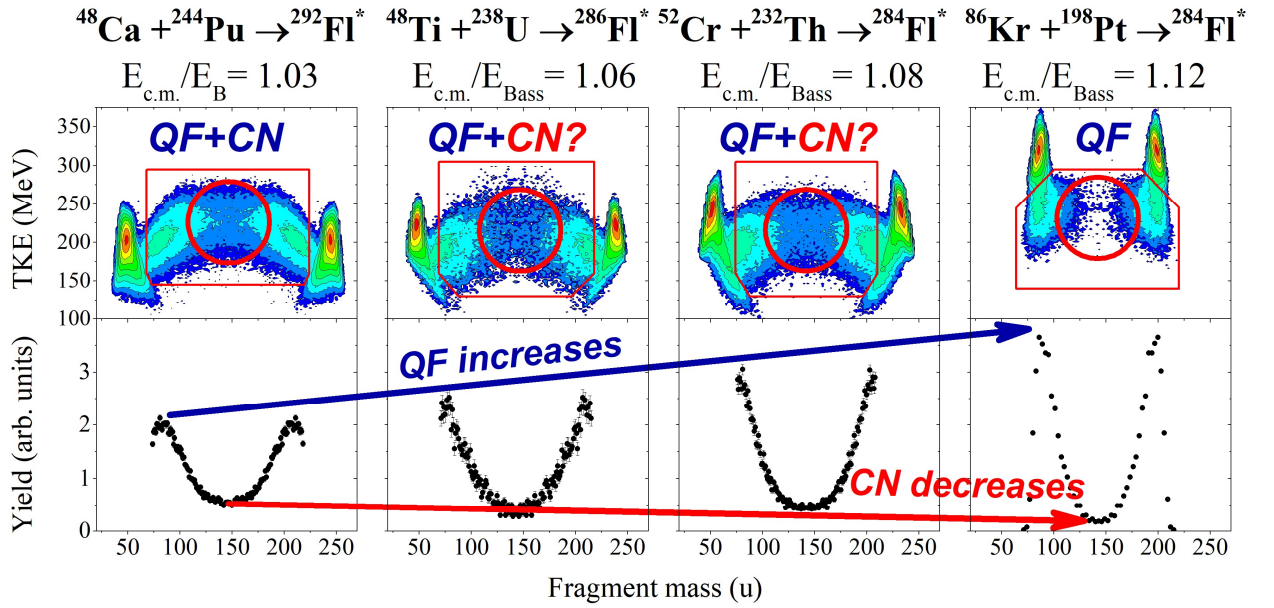


Fig. 12. Top panel: mass-energy distributions of binary fragments formed in the reactions $^{48}\text{Ca} + ^{244}\text{Pu}$, $^{48}\text{Ti} + ^{238}\text{U}$, $^{52}\text{Cr} + ^{232}\text{Th}$, and $^{86}\text{Kr} + ^{198}\text{Pt}$ leading to the formation of composite systems with $Z = 114$ at energies above the Bass barrier; bottom panel: mass distributions for fission-like fragments inside the contour line on M - TKE matrices.

The investigations showed that in the case of the reactions with Ti and Cr ions the properties of asymmetric QF fragments are similar to those obtained in the reactions with ^{48}Ca ions with the reaction time of about 5–7 zs. Moreover, shorter reaction times of about 3 zs were observed in the case of Ni and Zn ions. From the comparison of mass and energy distributions and capture cross sections, it was found that the contribution of QF fragments formed in long-lived composite systems decreases sharply at the transition from systems with $Z_1Z_2 \approx 2300$ ($^{52}\text{Cr} + ^{232}\text{Th}$, $^{52,54}\text{Cr} + ^{248}\text{Cm}$) to those with $Z_1Z_2 > 2500$ ($^{86}\text{Kr} + ^{198}\text{Pt}$, $^{68}\text{Zn} + ^{232}\text{Th}$), and the main reaction channels were shown to be a few-nucleon transfer and deep inelastic collisions.

The fusion probabilities for studied reactions were estimated on the basis of the analysis of mass and TKE distributions. The obtained fusion probabilities are in good agreement with the

fusion probability dependence on the mean fissility parameter found for the reactions of well-deformed nuclei with ^{36}S , ^{48}Ca , ^{48}Ti , and ^{64}Ni ions. The fusion probability is found to drop by approximately three orders of magnitude at the transition from $^{48}\text{Ca} + ^{238}\text{U}$ to the $^{54}\text{Cr} + ^{248}\text{Cm}$ reaction and by more than a factor of 10^5 to the $^{68}\text{Zn} + ^{232}\text{Th}$ reaction at energies above the Coulomb barrier. Based on the obtained fusion probability for the $^{54}\text{Cr} + ^{248}\text{Cm}$ reaction, the production cross section of superheavy element with $Z = 120$ is expected to be about a few femtobarns. In the case of the $^{64}\text{Ni} + ^{238}\text{U}$ and $^{68}\text{Zn} + ^{232}\text{Th}$ reactions the production cross sections are one and two orders of magnitude lower, respectively.

Unfortunately, in the complete fusion reactions superheavy nuclei cannot reach the predicted neutron closed shell with $N = 184$ due to the lack of 7–9 neutrons. It was proposed to use multinucleon transfer reactions, in particular, inverse QF to produce new neutron-rich heavy and superheavy nuclei at bombarding energies close to the Coulomb barrier.

In 2017, the influence of the closed shells on the formation of inverse QF fragments has been studied. The mass, energy and angular distributions of fragments formed in the reactions $^{156,160}\text{Gd} + ^{186}\text{W}$ at $E_{\text{lab}} = 878$ MeV in the case of ^{156}Gd ions and $E_{\text{lab}} = 860, 935$ MeV for ^{160}Gd ions have been measured to study the influence of the closed proton and neutron shells on the formation of reaction products in the inverse QF process [26]. The enhanced yield of products with masses 200–215 u (mass transfer of 20–25 nucleons) was observed for both reactions $^{156,160}\text{Gd} + ^{186}\text{W}$ at energies near the Coulomb barrier. The cross sections of the formation of trans-target fragments heavier than 200 u in the reactions $^{156,160}\text{Gd} + ^{186}\text{W}$ at this energy are found to be about 10 μb . Although the formation cross sections of these fragments are approximately the same for both reactions, in the case of the ^{160}Gd -induced reaction the excitation energy is 10–20 MeV lower than in the case of ^{156}Gd . It leads to the less number of neutrons emitted during the deexcitation process in the former reaction. Thus, the reaction with ^{160}Gd ions is more suitable for producing neutron-rich nuclei in inverse QF process.

The orientation effect caused by the strong deformation of colliding nuclei plays an important role in the formation of the reaction fragments that can give a gain in the yield of trans-target fragments. The analysis of mass, energy and angular distributions of fragments formed in the reaction $^{160}\text{Gd} + ^{186}\text{W}$ at an energy of 935 MeV, which is above the barrier for side-to-side collisions and all the orientations of interacting nuclei are possible, has shown that the formation cross section of fragments with mass ~ 208 u is about 50 times higher than in the case of measurements at near the Coulomb barrier energy, while the excitation energies of these fragments, on average, increase insignificantly.

This enhancement found in the yield of products with masses heavier than the target mass confirms the important role of nuclear shells in inverse QF process in low-energy damped

collisions. Thereby, low-energy multinucleon transfer reactions are a promising pathway for producing new neutron-rich isotopes.

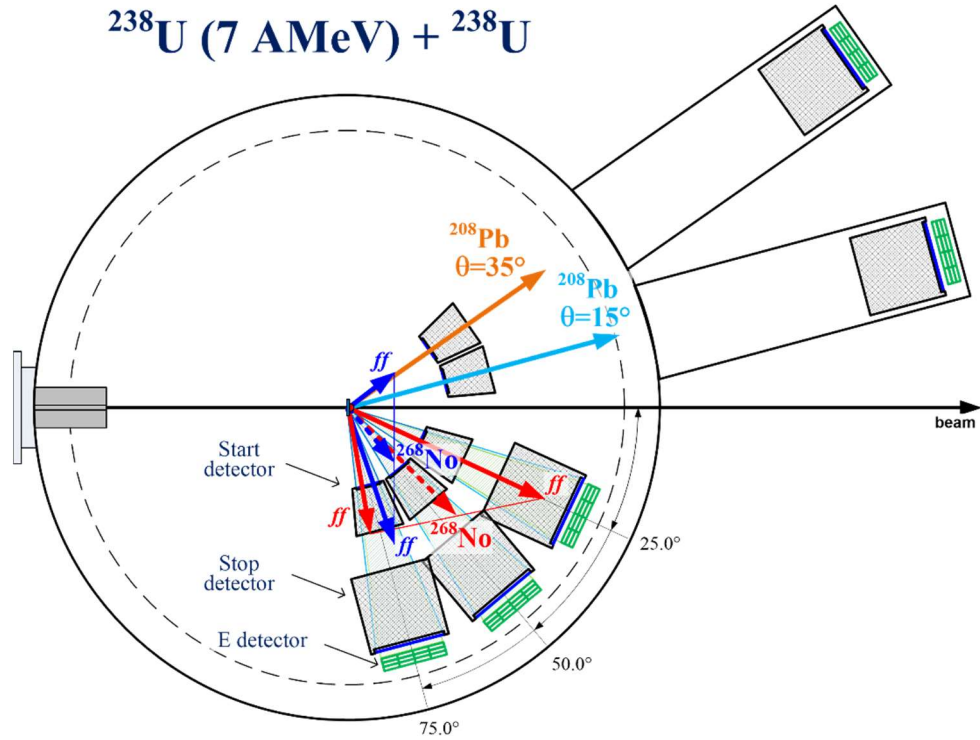


Fig. 13. Scheme of the CORSET setup to measure the formation of $^{208}\text{Pb} + ^{268}\text{No}$ fragments in multinucleon transfer process in the reaction $^{238}\text{U} + ^{238}\text{U}$ at the interaction energy of 7 AMeV. The orange and red arrows show the velocity vectors for the formation of Pb + No pair at an angle of 35° for Pb fragment, the light blue and blue arrows correspond to the case of an angle of 15° for Pb fragment.

In the nearest future, we plan to study the multinucleon transfer in the $^{238}\text{U} + ^{238}\text{U}$ reaction at an energy above the barrier for side-to-side collisions. At the first step of the investigations the probability of the $^{208}\text{Pb} + ^{268}\text{No}$ pair formation will be studied. According to the calculations of Karpov, the formed fragments of ^{268}No should have excitation energy up to a from 40 to 150 MeV and undergo fission during deexcitation process. In order to detect the binary channel $^{238}\text{U} + ^{238}\text{U} \rightarrow ^{208}\text{Pb}^* + ^{268}\text{No}^*$ as well as $^{208}\text{Pb}^* +$ fragments from the sequential fission of $^{268}\text{No}^*$ we installed five ToF-E arms inside the CORSET chamber. Such geometry allows reconstructing the full kinematics of formed fragment pairs even in the case of the sequential fission of No fragments. The geometry of the experiment is shown in Fig. 13.

The dynamical model of nucleus-nucleus collisions of heavy ions has been developed. The model allows one to describe all major regularities of multinucleon transfer reactions [27]. A possibility of synthesis of new neutron-rich isotopes of heavy elements in deep inelastic collisions

has been studied. The analysis of near barrier collisions of heavy spherical nuclei has shown that this type of reactions is a perspective one for synthesis of new nuclei. In particular, the predicted cross sections for production of new neutron-rich isotopes ^{201}Re and ^{200}W (having $N=126$) in the $^{136}\text{Xe} + ^{198}\text{Pt}/^{208}\text{Pb}$ reactions exceed 100 nb (Fig. 14).

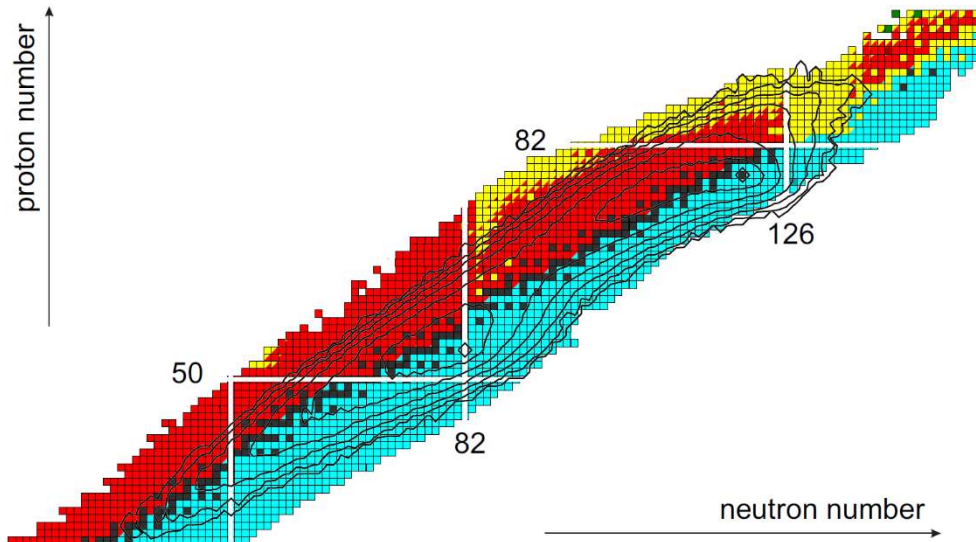


Fig. 14. The upper part of nuclear chart of known nuclides. The contour lines show the yields of products for the reaction $^{136}\text{Xe} + ^{198}\text{Pt}$ at $E_{c.m.} = 643 \text{ MeV}$. The contour lines are drawn over each order of magnitude of the cross section down to 100 nb.

The theoretical approach based on the Langevin equations has been extended to the case of reactions involved statically deformed nuclei [28]. Low-energy multinucleon transfer reactions in collisions of two actinide nuclei were modeled. Yields of nuclei heavier than the target were measured. The cross sections for the synthesis of such nuclei were shown to decrease rapidly as the number of transferred nucleons increased. This makes the region of superheavy nuclei hardly accessible via multinucleon transfer reactions. Quite high cross sections (those exceeding $1 \mu\text{b}$) nevertheless allow the synthesis of numerous as-yet-undiscovered isotopes of heavy actinides. (Fig. 15). The contour lines in the figure are drawn over each order of magnitude up to 1 pb.

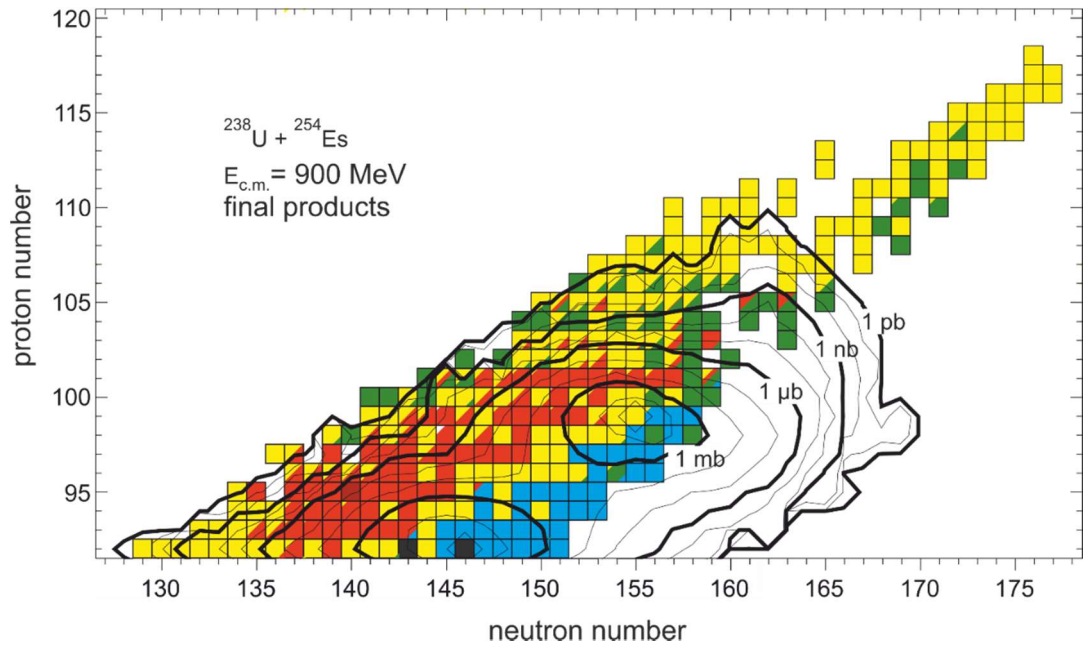


Fig. 15. Cross sections for the synthesis of nuclei in the $^{238}\text{U} + ^{254}\text{Es}$ reaction at the energy $E_{c.m.} = 900 \text{ MeV}$

NUCLEI AT STABILITY LIMITS

The flagship experiment performed at the ACCULINNA-2 facility was dedicated to extremely neutron-rich system ^7H and investigation of correlations between its $^3\text{H}+4\text{n}$ decay products. The ^7H ground state, which can decay via the unique five-body ($^3\text{H}+4\text{n}$) channel was not studied before. It is apparent that the best approach to populate the unstable ^7H nucleus is the $^8\text{He}(^2\text{H},^3\text{He})^7\text{H}$ reaction in inverse kinematics. Two experimental studies with detector systems covering different kinematical regions (see Fig. 16) were performed in 2018 and 2019, and, as a result, new information on the ^7H ground and first excited states was obtained [29, 30].

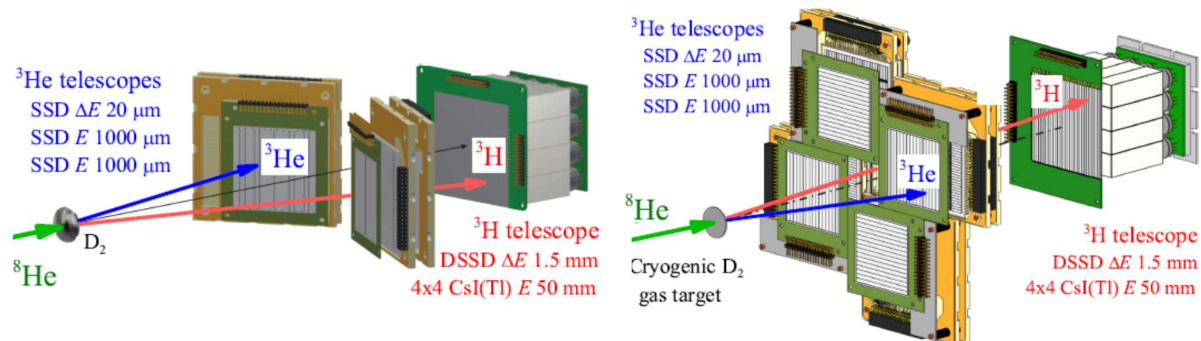


Fig. 16. Schematic view of telescopes dedicated to registration of products of the $^2\text{H}(^8\text{He},^3\text{He})^7\text{H}$ reaction at the ACCULINNA-2 facility employed in 2018 (left) and 2019 (right). The energy of ^8He beam was 26 MeV/nucleon in both runs.

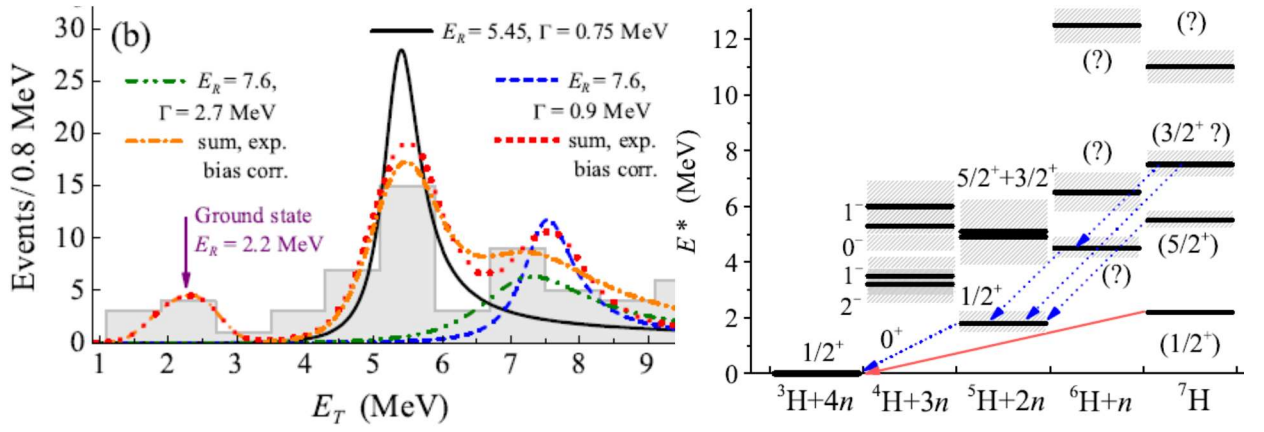


Fig. 17. Left panel: the energy profile of the ground state at 2.2(5) MeV and first excited states at 5.5(3) and 7.5(3) MeV obtained in the ${}^2\text{H}({}^8\text{He}, {}^3\text{He}){}^7\text{H}$ reaction [30]; the experimental missing mass spectrum of ${}^7\text{H}$ is shown by gray histogram. Right panel: the ${}^7\text{H}$ level scheme and the decay mechanism of the ground state via true $4n$ emission (red arrow) and the first excited states as the sequential $2n+2n$ emission or $n+2n$ via the ${}^5\text{H}$ and ${}^6\text{H}$ states, respectively (blue arrows).

In the first experiment [29,31], the resonant structure at $E_T = 6.5(5)$ MeV was observed (E_T is the energy above ${}^3\text{H}+4n$ threshold). It may be interpreted either as one state or as an overlapping doublet of $3/2^+$ and $5/2^+$ states. Moreover, a group of events at ~ 2 MeV was identified and indicated as a candidate for the ${}^7\text{H}$ $1/2^+$ ground state at $E_T = 1.8(5)$ MeV. However, due to the low statistics (5 events), there was incomplete confidence in the latter interpretation. The estimated cross section of the reaction channel populating this possible state appeared to be quite low: the value $d\sigma/d\Omega_{\text{c.m.}} \sim 25 \mu\text{b/sr}$ was derived for the reaction angle in the range $19^\circ - 27^\circ$.

The second experiment carried out in 2019 [30] took advantage of refactored, and improved telescopes for detection of ${}^3\text{He}$. The modified setup has larger solid angle and covered smaller reaction angles. The accumulated number of ${}^7\text{H}$ events in the new experiment was more than three times larger in comparison with the first one [29]. In addition, calibration of the ${}^7\text{H}$ missing mass spectrum was independently verified by measurement of the missing mass of ${}^9\text{Li}$ populated in the ${}^{10}\text{Be}({}^2\text{H}, {}^3\text{He}){}^9\text{Li}$ reaction at the beam energy 42 MeV/nucleon. Reliable experimental evidence for the population of two resonant states in ${}^7\text{H}$ at 2.2(5) and 5.5(3) MeV relative to ${}^3\text{H}+4n$ threshold was observed in [30], see Fig. 17. Moreover, some evidence for the resonant state at 7.5(3) was present in the missing mass spectrum. Basing on the energy and angular distributions, one may argue that the weakly populated 2.2(5) MeV peak is the ${}^7\text{H}$ $1/2^+$ ground state. It is highly plausible that the newly ascertained position of the state at 5.5(3) MeV is the $5/2^+$ member of the ${}^7\text{H}$ excitation doublet, built on the 2^+ state of valence neutrons. A possible explanation of the 7.5 MeV state may be that it is the $3/2^+$ member of the $5/2^+$ & $3/2^+$ doublet of the excited states, which could

not be resolved earlier [29] because of worse energy resolution. In summary, the ${}^7\text{H}$ level scheme and the decay mechanism of the ground and first excited states was proposed (Fig.17, right panel).

The other experiment performed at the ACCULINNA-2 fragment separator was aimed at the study of low-lying states of ${}^{10}\text{Li}$ system produced in the ${}^9\text{Li}(d,p){}^{10}\text{Li}$ reaction in inverse kinematics with subsequent decay ${}^{10}\text{Li} \rightarrow n+{}^9\text{Li}$ with the ${}^9\text{Li}$ beam energy of 29 MeV/nucleon [32], see Fig. 18. The experimental resolution of the whole setup was checked, normalizing of ${}^{10}\text{Li}$ missing mass spectra by means of the reference ${}^6\text{He}(d,p){}^7\text{He}$ reaction where triple coincidences p - ${}^6\text{He}$ - n were measured. Taking into account the collected statistics (about 400 triple coincidences p - ${}^9\text{Li}$ - n), and good energy resolution of ~ 250 keV (FWHM) of the ${}^{10}\text{Li}$ spectrum, one can assume to get new data on low-lying ${}^{10}\text{Li}$ states at ~ 0.5 and ~ 4 MeV. Later in 2020, the method [32] of triple coincidence p - n -core was applied for study of ${}^9\text{He}$ in the ${}^8\text{He}(d,p){}^9\text{He}$ reaction. The data analysis is in progress.

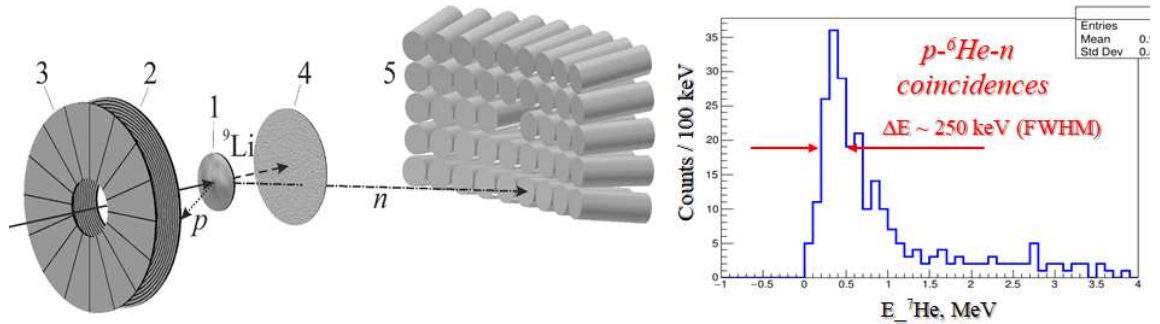


Fig. 18. Left panel: scheme of the experimental setup for ${}^{10}\text{Li}$ and ${}^{7,9}\text{He}$ study using (d,p) reaction; 1 – cryogenic deuterium target, 2 - double-side Si strip detector, 3 – Si veto detector, 4 - thin plastic scintillator, 5 - neutron detectors array. Right panel: experimental energy resolution obtained in the reference ${}^6\text{He}(d,p){}^7\text{He}$ reaction at $E({}^6\text{He}) = 29$ MeV/nucleon.

The first joint experiment at ACCULINNA-2 with the group from the Warsaw University was carried out in 2020. Rare decay channels of the neutron-deficient ${}^{26}\text{P}$ and ${}^{27}\text{S}$ nuclei (beta-delayed emission of one, two and even three protons) were investigated using the optical time projection chamber. The high quality of the identification of the radioactive beam particles achieved at the ACCULINNA-2 separator (Fig. 19), using the standard time-of-flight and energy loss measurements, provided high-statistics data. The analysis will allow obtaining new information on the decay of these nuclei via the βp , $\beta 2p$, and $\beta 3p$ channels. The quality of the data is significantly better in comparison with the previous one obtained earlier by the same technique at the ACCULINNA-1 setup [33].

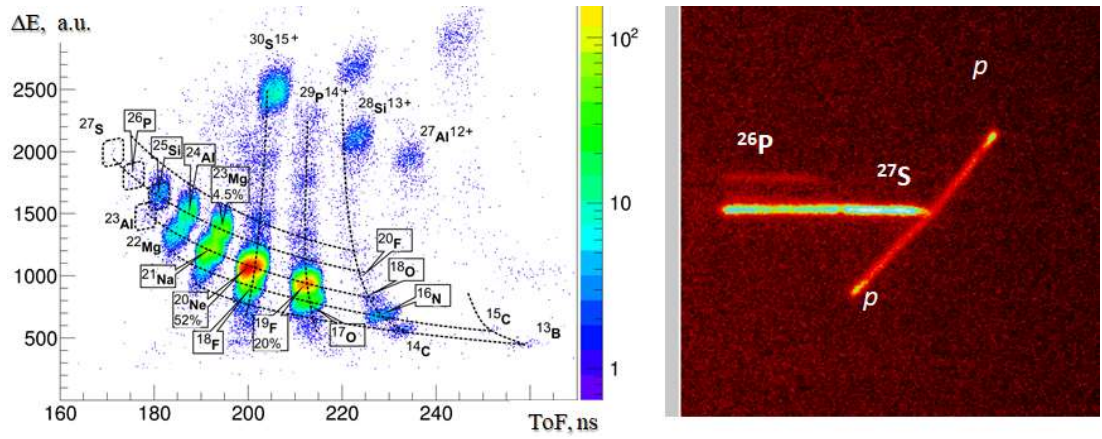


Fig. 19. Identification of proton-rich isotopes when the ACCULINNA-2 separator was adjusted to the maximum yield of the ^{26}P and ^{27}S ions in fragmentation of ^{32}S (51.5 MeV/nucleon) on the Be target (left) and the example of two-proton beta-delayed events of the ^{27}S isotope (right).

A new method was developed for determining the spectrum of excited states of the ^{17}Ne nucleus undergoing $2p$ -decay [34]. The method was applied for analysis of the $3/2^-$ -state of the ^{17}Ne nucleus populated in the reaction $^{18}\text{Ne}(p,d)^{17}\text{Ne}$ in inverse kinematics. The experiment was carried out at the ACCULINNA-1 facility with ^{18}Ne secondary beam at the 35 MeV/nucleon energy. A new limit for the ratio of the widths $\Gamma_{2p}/\Gamma_\gamma < 1.6 \times 10^{-4}$ was established. The obtained limit is ~ 50 times lower than the result obtained at MSU [Chromik et al., Phys. Rev. C **66** (2002) 024313]. The data obtained at ACCULINNA-1 are important for astrophysical application to perform calculations describing the origin of elements in the Universe. They also provide a way to employ the possibility of radiation capture of the proton pair by the ^{15}O nucleus which is the so-called "waiting point" in the astrophysical rp -process. Additionally, the data allow to excluding from consideration the application of the simplified diproton decay model used earlier to estimate the ratio of $2p$ and gamma-decays widths.

Three-body p - p - ^4He continuum from the $^6\text{Li}(p,n)^6\text{Be}$ charge-exchange reaction in inverse kinematics was studied in detail [35,36]. Very high statistics (~ 4.7 millions of events) was collected earlier at ACCULINNA-1 [A. Fomichev et al., Phys. Lett. B **708** (2012) 6], and the corresponding analysis of three-body correlations was performed. A theoretical model combining plane wave impulse approximation and hyperspherical harmonics method describing the population of ^6Be in charge-exchange reaction with its subsequent three-body decay was developed. Data generated by this model were used as input for very detailed simulation of the experiment, and experimental spectra were directly compared with the different configurations of the theoretical model. As a result, detailed information on both the structure of ^6Be and the charge-exchange reaction mechanism was extracted. The approach described in [35,36] was proposed as

a general tool for studying the internal and external correlations of a three-body continuum with broad overlapping states.

The EXPERT (EXotic Particle Emission and Radioactivity by Tracking) facility is designed for pioneering studies of nuclear systems located in the vicinity and far beyond the driplines, and thus decaying via the emission of one or several nucleons [37]. The project is developed as part of the FAIR international center (Darmstadt, Germany). The analysis of data obtained in experiments performed on the FRS fragment separator (GSI, Darmstadt) by the EXPERT collaboration was continued. The spectroscopy of excited states of unbound nuclei ^{30}Ar and ^{29}Cl was analyzed in [38] and the discovery of a new extremely proton-rich isotope ^{31}K was reported in [39]. This nuclear system was populated in a charge-exchange reaction with ^{31}Ar beam and a very exotic form of decay – emission of three protons was identified. Deep excursion beyond proton dripline and possibilities of EXPERT setup for nuclear structure study of extremely exotic systems were presented in review articles [40] and [41].

Theoretical studies on the development of the methods of the quantum-mechanical few-body problem, studies of decays and reactions of exotic nuclear systems near and beyond of limits of nuclear stability were carried out in [42-46]. In particular, an important theoretical problem, which is directly related to the ^7H experiment, is the study of correlations in systems, decaying into 5 particles. For first time, the possible correlations in the “true” 5-particle decays of systems like core+4n or core+4p were studied in [42]. It is known that in such systems there are complex spatial correlations (the so-called “Pauli focusing”) associated with the population of certain shell configurations. These correlations, existing in the nuclear interior region, can manifest themselves asymptotically in the decay correlations. It was also demonstrated that it is possible to extract information about the shell structure of nuclei having a core+4n structure by using all possible sets of two-dimensional angular correlations of the decay products.

Techniques for studies of the three-body nonresonant radiative captures for nuclear astrophysics were developed. Here, fundamentally important results were obtained by the examples of “benchmark” nonresonant reactions $^4\text{He}+n+n \rightarrow ^6\text{He}+\gamma$ [24] and $^{15}\text{O}+p+p \rightarrow ^{17}\text{Ne}+\gamma$ [44,45]. For the reactions of two-neutron capture, the correct low-energy E1 strength function was obtained for the first time, and the dominance of dineutron dynamics in the energy region, which is essential for problems of nuclear astrophysics, was demonstrated [43]. A fully analytical formalism, which is an analogue of the method of asymptotic normalization coefficients [44], was for the first time developed for reactions of the two-proton radiative capture. Theoretical studies of the soft dipole mode in three-particle core+n+n systems were continued. Fundamentally

important results were obtained for the ${}^6\text{He}$ system, in particular, high-precision calculations made it possible to solve the problem of the unstable “wavy” behavior of the E1 strength function [46].

REACTIONS WITH BEAMS OF LIGHT STABLE AND RADIOACTIVE NUCLEI

In 2019 most of the interest centered on the investigation of various reaction mechanisms leading to the formation of neutron-rich nuclei. Experiments were performed at heavy-ion accelerators in wide energy ranges, which was key in determining the channels of nuclear processes – from nucleon transfer reactions to fragmentation. The magnetic spectrometer MAVR in Dubna and the LISE facility in France were employed. An interesting result was obtained for the reaction with ${}^{18}\text{O}$ nuclei accelerated to 8.5 MeV/A and directed onto a ${}^{238}\text{U}$ target. A significant increase in the cross section for the production of exotic nuclei was detected owing to the transfer of a large number of neutrons from the target nucleus to the nucleus of the bombarding particle.

The collision dynamics of exotic nuclei was studied on the basis of the numerical solution of the time-dependent Schrödinger equation taking into account spin-orbital interaction [47]. The cross sections for nucleon transfer and break-up were calculated as the main components of the total cross section of the reaction with weakly bound nuclei studied at FLNR JINR experiments for the ${}^{11}\text{Li}+{}^{28}\text{Si}$, ${}^3\text{He}+{}^{194}\text{Pt}$, ${}^{45}\text{Sc}$, ${}^6\text{He} + {}^{197}\text{Au}$, and ${}^9\text{Li} + {}^{28}\text{Si}$ reactions (Fig. 20).

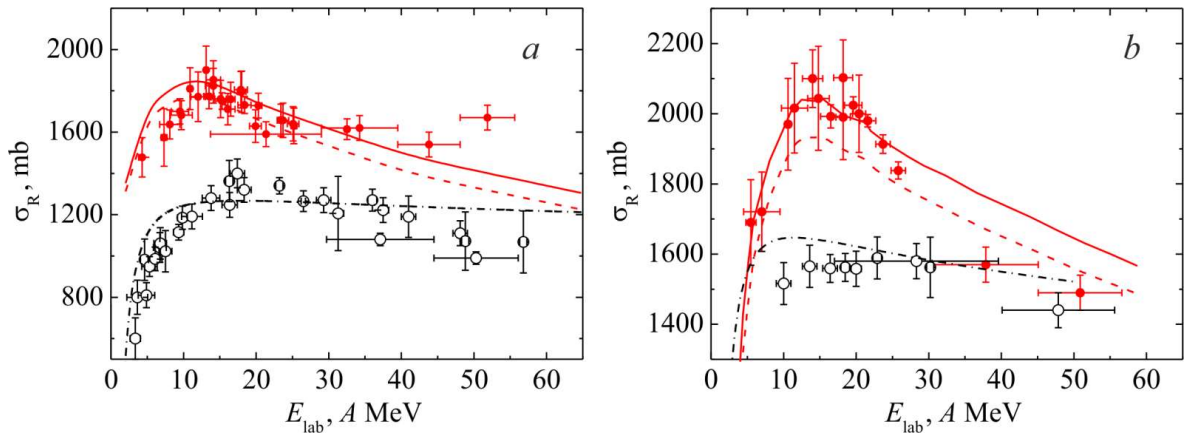


Fig. 20. Fig. The excitation function for ${}^{4,6}\text{He} + \text{Si}$ (a) and ${}^{7,9}\text{Li} + \text{Si}$ (b). Dashed lines show calculations using the time-dependent Schrödinger equation.

The manifestation of clustering in light atomic nuclei was studied with reference to deuteron reactions with ${}^9\text{Be}$ nuclei at low energies [48]. The folding atomic nuclei potential was calculated on the basis of a three-cluster model with the nucleus ${}^9\text{Be} = n + \alpha + \alpha$. The main reaction channels, including those involving the transfer of large clusters, were analyzed within the framework of the coupled-channels model. In particular, the ${}^9\text{Be}(d, \alpha){}^7\text{Li}$ reaction channel accompanied by the ${}^5\text{He}$

cluster transfer was found to give a significant contribution to the cross section in the low collision energy domain, which is confirmed by the data from previous experiments.

In 2020, experiments using the new high-resolution magnetic analyzer (MAVR set-up) were launched. Experiments aimed at measuring the energy spectra of alpha particles in a wide energy range were carried out at the U-400 heavy-ion cyclotron.

The reactions with the ^{48}Ca and ^{56}Fe beams accelerated to 6 MeV per nucleon and ^{238}U and ^{181}Ta targets were studied. The differential cross sections for the emission of alpha particles at 0° were measured as a function of their energy (Fig. 21). Fast alpha particles at energies corresponding to the two- and three-body reaction channels, including those with energies close to the two-body kinematic limit, were observed in the recorded spectra.

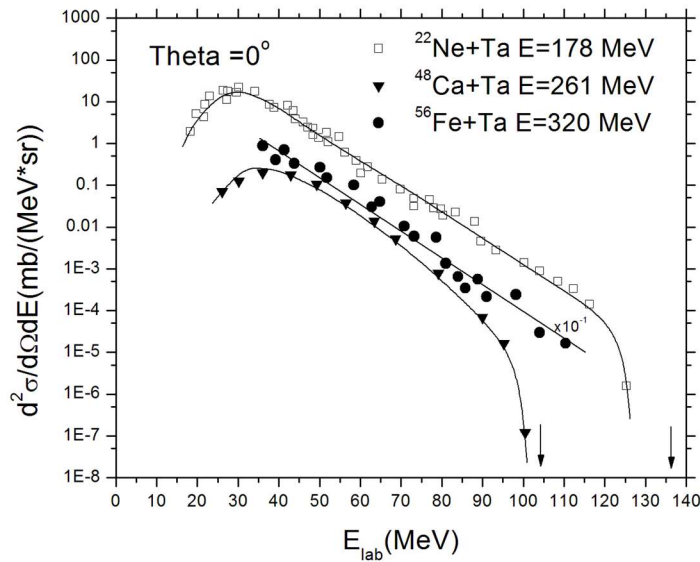


Fig. 21. Energy spectra of alpha particles measured at 0° in reactions with the ^{181}Ta target using different projectiles: ^{56}Fe at 320 MeV (circles), ^{22}Ne at 180 MeV (squares), and ^{48}Ca at 270 MeV (triangles). The arrows show the energies of alpha particles corresponding to the kinematic limit of the two-body reaction channels using ^{48}Ca (left arrow) and ^{22}Ne (right arrow) nuclei.

The analysis of the experimental data conducted within the model of moving sources revealed several sources of fast alpha particles. The energy spectra of alpha particles were shown to be mainly characterized by the properties of heavy target nuclei and, to a lesser extent, by the properties of incident beam nuclei.

The investigations of the total cross sections for the reactions of the ^6He , ^8He , and ^9Li beams with the ^{28}Si , ^{59}Co , and ^{181}Ta targets were pursued. The energy dependence of the total cross sections, $\sigma_{\text{R}}(E)$, for the reactions was measured in the range of 20–40 MeV per nucleon. The cross

sections for the interaction of ${}^6\text{He}$, ${}^8\text{He}$, and ${}^9\text{Li}$ with ${}^{59}\text{Co}$ and ${}^{181}\text{Ta}$ were measured for the first time. The measurements were carried out using the 4π γ -ray MULTI spectrometer comprising 12 CsI (Tl) and nine CeBr3 scintillation detectors that have high γ -ray detection efficiency in a wide energy range. On the basis of a newly developed method for experimental data analysis, we obtained the total cross sections σ_R and their distribution over the γ -ray multiplicity [48].

KNOWLEDGEBASE ON LOW-ENERGY NUCLEAR PHYSICS

The NRV web knowledge base on low-energy nuclear physics (<http://nrv.jinr.ru/>) has been developed in the Joint Institute for Nuclear Research [49]. It integrates a large amount of experimental data with computational codes for modeling of nuclear properties and nuclear reactions. It also provides possibilities for planning experiments and analysis of experimental data. The knowledge base is available for any remote user via any web browser supporting the Java plugin. The main focus of the system is on modeling of nuclear reactions: elastic and inelastic scattering, nucleon transfer, fusion with subsequent decay of the excited compound nucleus, etc. The NRV knowledge base may be used for both scientific and educational purposes.

Further use of the current version of the system is limited by the fact that there are trends of gradual drop of support of the Java plugins (and, hence, Java applets) by the new versions of browsers. Thus, the further development of the NRV knowledge base is focused on the modernization of the user interface, in particular, a transition from the use of Java applets to the use of new technologies, such as HTML5 and JavaScript. The current version of a new version of the system can be accessed via <http://nrv2.jinr.ru>. In parallel, we have developed a special browser supporting Java applets in order to preserve the possibility of using the current version of NRV. The browser is available for Windows and Linux OS and can be download from <http://nrv.jinr.ru/>.

In total, the results obtained under the theme 1130 (2017-2021) were published in 235 scientific papers.

MAIN REFERENCES

- [1] V.K. Utyonkov, N.T. Brewer, Yu.Ts. Oganessian, K.P. Rykaczewski, F.Sh. Abdullin, S.N. Dmitriev, R.K. Grzywacz, M.G. Itkis, K. Miernik, A.N. Polyakov, J.B. Roberto, R.N. Sagaidak, I.V. Shirokovsky, M.V. Shumeiko, Yu.S. Tsyganov, A.A. Voinov, V.G. Subbotin, A.M. Sukhov, A.V. Karpov, A.G. Popeko, A.V. Sabel'nikov, A.I. Svirikhin, G.K. Vostokin, J.H. Hamilton, N.D. Kovrizhnykh, L. Schlattauer, M.A. Stoyer, Z. Gan, W.X. Huang, L. Ma., Neutron-deficient superheavy nuclei obtained in the $^{240}\text{Pu}+^{48}\text{Ca}$ reaction. *Phys. Rev. C* 97, 014320-1-10 (2018).
- [2] Gennadii Ya. Starodub, Yury S. Tsyganov, Vladimir K. Utyonkov, Alexey A. Voinov, Grigory K. Vostokin, Alexander V. Yerebin, and Sergey N. Dmitriev., On the volatility of nihonium (Nh, $Z = 113$). *Eur. Phys. J. A* 53, 158 (2017).
- [3] V.K. Utyonkov, Yu.Ts. Oganessian, S.N. Dmitriev, M.G. Itkis, K.J. Moody, M.A. Stoyer, D.A. Shaughnessy, J.B. Roberto, K.P. Rykaczewski, J.H. Hamilton for the collaboration. Discovery of elements 113 to 118. *Eur. Journal of Physics and Functional Materials* 1(1), 5-11 (2017).
- [4] N.T. Brewer, V.K. Utyonkov, K.P. Rykaczewski, Yu.Ts. Oganessian, F.Sh. Abdullin, R.A. Boll, D.J. Dean, S.N. Dmitriev, J.G. Ezold, L.K. Felker, R.K. Grzywacz, M.G. Itkis, N.D. Kovrizhnykh, D. C. McInturff, K. Miernik, G.D. Owen, A.N. Polyakov, A.G. Popeko, J.B. Roberto, A.V. Sabel'nikov, R.N. Sagaidak, I.V. Shirokovsky, M.V. Shumeiko, N.J. Sims, E.H. Smith, V.G. Subbotin, A.M. Sukhov, A.I. Svirikhin, Yu.S. Tsyganov, S.M. Van Cleve, A.A. Voinov, G.K. Vostokin, C.S. White, J.H. Hamilton, and M. A. Stoyer., Search for the heaviest atomic nuclei among the products from reactions of mixed-Cf with a ^{48}Ca beam. *Phys. Rev. C* 98, 024317 (2018).
- [5] Zhishuai Ge, Cheng Li, Jingjing Li, Gen Zhang, Bing Li, Xinxin Xu, Cheikh A. T. Sokhna, Xiaojun Bao, Yu.S. Tsyganov, and Feng-Shou Zhang. Effect of shell corrections on the α -decay properties of $^{280-305}\text{Fl}$ isotopes. *Physical Review C* 98, 034312 (2018).
- [6] Jingjing Li, Cheng Li, Gen Zhang, Bing Li, Xinxin Xu, Zhong Liu, Yu. S. Tsyganov, and Feng-Shou Zhang. Theoretical study on production of unknown neutron-deficient $^{280-283}\text{Fl}$ and neutron-rich $^{290-292}\text{Fl}$ isotopes by fusion reactions. *Phys. Rev. C* 98, 014626 (2018).
- [7] R.N. Sagaidak, N.A. Kondratiev, L. Corradi, E. Fioretto, T. Mijatovic, G. Montagnoli, F. Scarlassara, A.M. Stefanini, S. Szilner. Charge distributions of Ra recoil ions produced in $^{12}\text{C} + \text{Pb}$ fusion-evaporation reactions. *Phys. Rev. C* 97 054622 (2018).

- [8] V.B. Zlokazov and V.K. Utyonkov. Reply to Comment on ‘Analysis of decay chains of superheavy nuclei produced in the $^{249}\text{Bk}+^{48}\text{Ca}$ and $^{243}\text{Am}+^{48}\text{Ca}$ reactions’. *J. Phys. G: Nucl. Part. Phys.* 46 (2019) 018002 (3pp).
- [9] Z.Y. Zhang, Z.G. Gan, H.B. Yang, L. Ma, M.H. Huang, C.L. Yang, M.M. Zhang, Y.L. Tian, Y.S. Wang, M.D. Sun, H.Y. Lu, W.Q. Zhang, H.B. Zhou, X. Wang, C.G. Wu, L.M. Duan, W.X. Huang, Z. Liu, Z.Z. Ren, S.G. Zhou, X.H. Zhou, H.S. Xu, Yu.S. Tsyganov, A.A. Voinov, and A.N. Polyakov. New Isotope ^{220}Np : Probing the Robustness of the $N = 126$ Shell Closure in Neptunium *Phys. Rev. Lett.* 122, 192503 (2019).
- [10] Zhishuai Ge, Gen Zhang, Shihui Cheng, Yuling Li, Ning Su, Wuzheng Guo, Yu. S. Tsyganov, Feng-Shou Zhang. Theoretical predictions for α -decay properties of $^{283-339}\text{Og}$ using a shell-effect induced generalized liquid-drop model. *Eur. Phys. J. A*, 55, 166 (2019).
- [11] R. N. Sagaidak, N. A. Kondratiev, L. Corradi, E. Fioretto, G. Montagnoli, F. Scarlassara, and A. M. Stefanini. Ranges of Rn evaporation residues produced in the $^{16}\text{O} + ^{194}\text{Pt}$ reaction. *Phys. Rev. C* 99, 014602 (2019)
- [12] Svirikhin A.I., Andreev A.V., Yeremin A.V., Zamyatin N.I., Izosimov I.N., Isaev A.V., Kuznetsov A.N., Kuznetsova A.A., Malyshev O.N., Popeko A.G., Popov Y.A., Sokol E.A., Tezekbayeva M.S., Chelnokov M.L., Chepigin V.I., Schneidman T.M., Andel B., Antalic S., Bronis A., Mosat P., Gall B., Dorvaux O., Retailleau B.M., Hauschild K., Lopez-Martenz A., Prompt Neutrons from Spontaneous ^{254}Rf Fission, *Physics of Particles and Nuclei Letters*. Volume 16. Issue 6. 1 November 2019. Pages 768-771. DOI: 10.1134/S1547477119060311
- [13] Lopez-Martens A., Hauschild K., Rezyunkina K., Yeremin A.V., Tezekbayeva M.S., Chelnokov M.L., Chepigin V.I., Gustova M.V., Isaev A.V., Karpov A.V., Kuznetsova A.A., Malyshev O.N., Popeko A.G., Popov Y.A., Svirikhin A.I., Sokol E.A., Steinegger P., Asfari Z., Brionnet P., Dorvaux O. et al., Measurement of proton-evaporation rates in fusion reactions leading to transfermium nuclei, *Physics Letters. Section B: Nuclear, Elementary Particle and High-Energy Physics*. 2019. T. 795. C. 271-276. DOI: 10.1016/j.physletb.2019.06.010.
- [14] Yeremin A.V., Popeko, A.G., Malyshev O.N., Isaev A.V., Kuznetsova A.A., Popov Y.A., Svirikhin A.I., Sokol E.A., Tezekbayeva M.S., Chelnokov M.L., Chepigin V.I., Lopez-Martens A., Hauschild K., Dorvaux O., Gall B., Piot J., Antalic S., Mosat P., Tonev D., Stefanova E., Spectroscopy of the Isotopes of Transfermium Elements in Dubna: Current Status and Prospects, *Physics of Atomic Nuclei*. Volume 83, Issue 4, 1 July 2020, Pages 503-512. DOI: 10.1134/S1063778820040109

- [15] K. Kessaci, B.J.P. Gall, O. Dorvaux, A. Lopez-Martens, R. Chakma, K. Hauschild, D. Ackermann, M.L. Chelnokov, V.I. Chepigin, M. Forge, A.V. Isaev, I.N. Izosimov, D.E. Katrasev, A.A. Kuznetsova, O.N. Malyshev, J. Piot, A.G. Popeko, Yu.A. Popov, E.A. Sokol, A.I. Svirikhin, A.V. Yeregin, Evidence of high-K isomerism in ^{256}No , (Submitted to Phys Rev. C)
- [16] Chakma R., Hauschild K., Lopez-Martens A., Yeregin A.V., Malyshev O.N., Popeko A.G., Popov Y.A., Svirikhin A.I., Chepigin V.I., Dorvaux O., Gall B., Kessaci K., Gamma and conversion electron spectroscopy using GABRIELA, European Physical Journal A. V. 56. Issue 10. 1 October 2020, Article number 245 DOI: 10.1140/epja/s10050-020-00242-5
- [17] N.V. Aksenov, P. Steinegger, F.Sh. Abdullin, Y.V. Albin, G.A. Bozhikov, V.I. Chepigin, R. Eichler, V.Ya. Lebedev, A.Sh. Madumarov, O.N. Malyshev, O.V. Petrushkin, A.N. Polyakov, Y.A. Popov, A.V. Sabel'nikov, R.N. Sagaidak, I.V. Shirokovsky, M.V. Shumeiko, G.Ya. Starodub, Y.S. Tsyganov, V.K. Utyonkov, A.A. Voinov, G.K. Vostokin, A.V. Yeregin, S.N. Dmitriev. On the volatility of nihonium (Nh, $Z = 113$) // Eur. Phys. J. A. 2017. V.53. 158. P.1-5.
- [18] P. Steinegger N. V. Aksenov, Y. V. Albin, G. A. Bozhikov, V. I. Chepigin, I. Chuprakov, S. N. Dmitriev, N. S. Gustova, A. Sh. Madumarov, O. N. Malyshev, Y. A. Popov, A. V. Sabelnikov, A. I. Svirikhin, M. G. Voronyuk, A. V. Yeregin, R. Eichler, D.P. Herrmann, P. Ionescu, B. Kraus, D. Piguet), B. Gall, Z. Asfari. Preparatory experiments for the chemical investigation of nihonium monohydroxide. LRC Annual Report 2017, (2018), pp. 12-13.
- [19] P. Steinegger, N. V. Aksenov, Yu. V. Albin, A. Y. Bodrov, G. A. Bozhikov, V. I. Chepigin, I. Chuprakov, S. N. Dmitriev, N. S. Gustova, A. V. Isaev, A. Sh. Madumarov, O. N. Malyshev, Y. Melnik, Yu. A. Popov, A. V. Sabelnikov, A. I. Svirikhin, M. G. Voronyuk, A. V. Yeregin, T. K. Sato, R. Dressler, R. Eichler, D. Herrmann, D. Piguet, P. Ionescu, B. Kraus, B. Gall, Z. Asfari. First results 2018/2019 from preparatory experiments with thallium. LRC Annual Report 2019, (2020), pp. 21-22.
- [20] N. M. Chiera, N. V. Aksenov, Y. V. Albin, G. A. Bozhikov, V. I. Chepigin, S. N. Dmitriev, R. Dressler, R. Eichler, V. Ya. Lebedev, A. Madumarov, O. N. Malyshev, D. Piguet, Y. A. Popov, A. V. Sabelnikov, P. Steinegger, A. I. Svirikhin, A. Turler, G. K. Vostokin, A. Vogege, A. V. Yeregin. Interaction of elemental mercury with selenium surfaces: model experiments for investigations of superheavy elements copernicium and flerovium // J. Radioanal. Nucl. Chem. 2017. V.311. P. 99–108.
- [21] B. Kraus, P. Steinegger, N.V. Aksenov, R. Dressler, R. Eichler, E. Griesmayer, D. Herrmann, A. Turler, C. Weiss. Charge carrier properties of single-crystal CVD diamond up to 473 K. Nuclear Inst. and Methods in Physics Research, A. 2021. 989. 164947.

- [22] E.M. Kozulin *et al.*, Features of the Fission Fragments Formed in the Heavy Ion induced $^{32}\text{S}+^{197}\text{Au}$ reaction near the interaction barrier. *Eur. Phys. J. A* 56, 6 (2020).
- [23] E. Vardaci *et al.*, Using γ rays to disentangle fusion-fission and quasifission near the Coulomb barrier: A test of principle in the fusion-fission and quasielastic channels. *Phys. Rev. C* 101, 064612 (2020).
- [24] E.M. Kozulin *et al.*, Fission and quasifission of the composite systems $Z=114$ formed in heavy-ion reactions at energies near the Coulomb barrier. *Phys. Rev. C* 99, 014616 (2019).
- [25] E. Vardaci, M. G. Itkis, I. M. Itkis, G. Knyazheva, E. M. Kozulin, Fission and quasifission toward the superheavy mass region. *J. Phys. G: Nucl. Part. Phys.* 46, 103002 (2019).
- [26] E.M. Kozulin *et al.*, Inverse quasifission in the reactions $^{156,160}\text{Gd}+^{186}\text{W}$. *Phys. Rev. C* 96, 064621 (2017).
- [27] A.V. Karpov and V.V. Saiko, Modeling near-barrier collisions of heavy ions based on a Langevin-type approach, *Phys. Rev. C* 96, 024618 (2017).
- [28] V.V. Saiko and A.V Karpov, Analysis of multinucleon transfer reactions with spherical and statically deformed nuclei by using a Langevin-type approach, *Phys. Rev. C* (2019).
- [29] A.A. Bezbakh, V. Chudoba, A.V. Gorshkov, S.A. Krupko, S.G. Belogurov, D. Biare, A.S. Fomichev, E.M. Gazeeva, L.V. Grigorenko, G.Kaminski, O. Kiselev, D.A. Kostyleva, I. Mukha, I.A. Muzalevskii, E.Yu. Nikolskii, Yu.L. Parfenova, A.M. Quynh, A. Serikov, S.I. Sidorchuk, P.G. Sharov, R.S. Slepnev, S.V. Stepantsov, A. Swiercz, P. Szymkiewicz, G.M. Ter-Akopian, R. Wolski, B. Zalewski, M.V. Zhukov, "Evidence for the first excited state of ^7H ", *Physical Review Letters* 124 (2020) 022502.
- [30] I.A. Muzalevskii, A.A. Bezbakh, E.Yu. Nikolskii, V. Chudoba, S.A. Krupko, S.G. Belogurov, D. Biare, A.S. Fomichev, E.M. Gazeeva, A.V. Gorshkov, L.V. Grigorenko, G. Kaminski, O. Kiselev, D.A. Kostyleva, M.Yu. Kozlov, B. Mauey, I. Mukha, Yu.L. Parfenova, W. Piatek, A.M. Quynh, V.N. Schetin, A. Serikov, S.I. Sidorchuk, P.G. Sharov, N.B. Shulgina, R.S. Slepnev, S.V. Stepantsov, A. Swiercz, P. Szymkiewicz, G.M. Ter-Akopian, R. Wolski, B. Zalewski, M.V. Zhukov, "Resonant states in ^7H . Experimental studies in the $^2\text{H}(^8\text{He}, ^3\text{He})$ reaction", *Physical Review C* 103 (2021) 044313.
- [31] I.A. Muzalevskii, V. Chudoba, S.G. Belogurov, A.A. Bezbakh, D. Biare, A.S. Fomichev, S.A. Krupko, E.M. Gazeeva, M.S. Golovkov, A.V. Gorshkov, L.V. Grigorenko, G. Kaminski, O. Kiselev, D.A. Kostyleva, M.Yu. Kozlov, B. Mauey, I. Mukha, E.Yu. Nikolskii, Yu.L. Parfenova, W. Piatek, A.M. Quynh, V.N. Schetin, A. Serikov, S.I. Sidorchuk, P.G. Sharov, R.S. Slepnev, S.V. Stepantsov, A. Swiercz, P. Szymkiewicz, G.M. Ter-Akopian, R. Wolski, B. Zalewski, "Detection of the low energy recoil ^3He in the reaction $^2\text{H}(^8\text{He}, ^3\text{He})^7\text{H}$ ", *Bulletin of the Russian Academy of Sciences: Physics*, 84 (2020) 500-504.

- [32] A.A. Bezbakh, S.G. Belogurov, D. Biare, V. Chudoba, A.S. Fomichev, E.M. Gazeeva, M.S. Golovkov, A.V. Gorshkov, G.Kaminski, S.A. Krupko, B. Mauey, I.A. Muzalevskii, E.Yu. Nikolskii, Yu.L. Parfenova, W. Piatek, A.M. Quynh, A. Serikov, S.I. Sidorchuk, P.G. Sharov, R.S. Slepnev, S.V. Stepantsov, A. Swiercz, P. Szymkiewicz, G.M. Ter-Akopian, R. Wolski, B. Zalewski, “Study of ^{10}Li low energy spectrum in the $^2\text{H}(^9\text{Li},p)$ reaction”, *Bulletin of the Russian Academy of Sciences: Physics*, 84 (2020) 491-494.
- [33] Ł. Janiak, N. Sokołowska, A.A. Bezbakh, A.A. Ciemny, H. Czyrkowski, R. Dabrowski, W. Dominik, A.S. Fomichev, M.S. Golovkov, A.V. Gorshkov, Z. Janas, G. Kaminski, A.G. Knyazev, S.A. Krupko, M. Kuich, C. Mazzocchi, M. Mentel, M. Pfützner, P. Plucinski, M. Pomorski, R.S. Slepnev, and B. Zalewski, “Beta-delayed proton emission from ^{26}P and ^{27}S ”, *Phys. Rev. C* 95 (2017) 034315, pp.1-9.
- [34] P.G. Sharov, A.A. Bezbakh, V. Chudoba, I.A. Egorova, A.S. Fomichev, M.S. Golovkov, T.A. Golubkova, A.V. Gorshkov, L.V. Grigorenko, G. Kaminski, A.G. Knyazev, S.A. Krupko, M. Mentel, E.Yu. Nikolskii, Yu.L. Parfenova, P. Pluchinski, S.A. Rymzhanova, S.I. Sidorchuk, R.S. Slepnev, S.V. Stepantsov, G.M. Ter-Akopian, R. Wolski, M.V. Zhukov, “Search for 2p decay of the first excited state of ^{17}Ne ”, *Phys. Rev. C* 96, (2017) 025807.
- [35] V. Chudoba, L.V. Grigorenko, A.S. Fomichev, A.A. Bezbakh, I.A. Egorova, A.S. Fomichev, S.N. Ershov, M.S. Golovkov, A.V. Gorshkov, V.A. Gorshkov, G. Kaminski, S.A. Krupko, I.G. Mukha, E. Yu. Nikolskii, Yu.L. Parfenova, S.I. Sidorchuk, P.G. Sharov, R.S. Slepnev, L. Standylo, S.V. Stepantsov, G.M. Ter-Akopian, R. Wolski, M.V. Zhukov, “Three-body correlations in direct reactions. Example of ^6Be populated in (p,n) reaction”, *Physical Review C* 98 (2018) 054612.
- [36] V. Chudoba, L.V. Grigorenko, A.S. Fomichev, A.A. Bezbakh, I.A. Egorova, S.N. Ershov, A.V. Gorshkov, V.A. Gorshkov, G. Kaminski, S.A. Krupko, I. Mukha, E.Yu. Nikolskii, Yu.L. Parfenova, S.I. Sidorchuk, P.G. Sharov, R.S. Slepnev, L. Standylo, S.V. Stepantsov, G.M. Ter-Akopian, R. Wolski, M.V. Zhukov, “Detailed Study of External Correlations in the Low-Energy Spectrum of Beryllium-6”, *Bull. Rus. Acad. Sci. Phys.* 83 (2019) 392.
- [37] V. Chudoba for the EXPERT project, “The EXPERT project: part of the Super-FRS Experiment Collaboration”, *J. Phys.: Conf. Ser.* 1024 (2018) 012021; <http://aculina.jinr.ru/expert.html>
- [38] X. Xu, I. Mukha, L.V. Grigorenko, C. Scheidenberger, L. Acosta, E. Casarejos, V. Chudoba, A.A. Ciemny, W. Dominik, J. Duenas-Diaz, V. Dunin, J.M. Espino, A. Estrade, F. Farinon, A. Fomichev, H. Geissel, T.A. Golubkova, A. Gorshkov, Z. Janas, G. Kaminski, O. Kiselev, R. Knobel, S. Krupko, M. Kuich, Yu.A. Litvinov, G. Marquinez-Duran, I. Martel, C. Mazzocchi, C. Nociforo, A.K. Orduz, M. Pfützner, S. Pietri, M. Pomorski, A. Prochazka, S.

- Rymzhanova, A.M. Sanchez-Benitez, P. Sharov, H. Simon, B. Sitar, R. Slepnev, M. Stanoiu, P. Strmen, I. Szarka, M. Takechi, Y.K. Tanaka, H. Weick, M. Winkler, J.S. Winfield, M.V. Zhukov, "Spectroscopy of Excited States of unbound nuclei ^{30}Ar and ^{29}Cl ", *Physical Review C* 97 (2018) 034305.
- [39] D. Kostyleva, I. Mukha, L. Acosta, E. Casarejos, V. Chudoba, A.A. Ciemny, W. Dominik, J.A. Duenas, V. Dunin, J.M. Espino, A. Estrade, F. Farinon, A. Fomichev, H. Geissel, A.V. Gorshkov, L.V. Grigorenko, Z. Janas, G. Kaminski, O. Kiselev, R. Knobel, S. Krupko, M. Kuich, Yu.A. Litvinov, G. Marquinez-Duran, I. Martel, C. Mazzocchi, C. Nociforo, A.K. Orduz, M. Pfutzner, S. Pietri, M. Pomorski, A. Prochazka, S. Rymzhanova, A.M. Sanchez-Benitez, C. Scheidenberger, H. Simon, B. Sitar, R. Slepnev, M. Stanoiu, P. Strmen, I. Szarka, M. Takechi, Y.K. Tanaka, H. Weick, M. Winkler, J.S. Winfield, X. Xu, and M.V. Zhukov, "Towards the Limits of Existence of Nuclear Structure: Observation and First Spectroscopy of the Isotope ^{31}K by Measuring Its Three-Proton Decay", *Phys. Rev. Lett.* 123 (2019) 092502.
- [40] I. Mukha, L.V. Grigorenko, D. Kostyleva, C. Scheidenberger, L. Acosta, E. Casarejos, V. Chudoba, A.A. Ciemny, W. Dominik, J. Duenas-Diaz, V. Dunin, J.M. Espino, A. Estrade, F. Farinon, A. Fomichev, H. Geissel, A. Gorshkov, Z. Janas, G. Kaminski, O. Kiselev, R. Knobel, S. Krupko, M. Kuich, Yu.A. Litvinov, G. Marquinez-Duran, I. Martel, C. Mazzocchi, C. Nociforo, A.K. Orduz, M. Pfutzner, S. Pietri, M. Pomorski, A. Prochazka, S. Rymzhanova, A.M. Sanchez-Benitez, P. Sharov, H. Simon, B. Sitar, R. Slepnev, M. Stanoiu, P. Strmen, I. Szarka, M. Takechi, Y.K. Tanaka, H. Weick, M. Winkler, J.S. Winfield, X. Xu, M.V. Zhukov, "Deep excursion beyond proton dripline. I. Argon and chlorine isotope chains", *Physical Review C* 98 (2018) 064308.
- [41] L.V. Grigorenko, I. Mukha, D. Kostyleva, C. Scheidenberger, L. Acosta, E. Casarejos, V. Chudoba, A.A. Ciemny, W. Dominik, J. Duenas-Diaz, V. Dunin, J.M. Espino, A. Estrade, F. Farinon, A. Fomichev, H. Geissel, A. Gorshkov, Z. Janas, G. Kaminski, O. Kiselev, R. Knobel, S. Krupko, M. Kuich, Yu.A. Litvinov, G. Marquinez-Duran, I. Martel, C. Mazzocchi, E.Yu. Nikolskii, C. Nociforo, A.K. Orduz, M. Pfutzner, S. Pietri, M. Pomorski, A. Prochazka, S. Rymzhanova, A.M. Sanchez-Benitez, P. Sharov, H. Simon, B. Sitar, R. Slepnev, M. Stanoiu, P. Strmen, I. Szarka, M. Takechi, Y.K. Tanaka, H. Weick, M. Winkler, J.S. Winfield, X. Xu, M.V. Zhukov, "Deep excursion beyond proton dripline. II. Towards the limits of nuclear structure existence in EXPERT setup", *Physical Review C* 98 (2018) 064309.
- [42] P.G. Sharov, L.V. Grigorenko, A. Ismailova, M.V. Zhukov, "Pauli-principle driven correlations in four-neutron nuclear decays", *JETP Letters* 110 (2019) 5-14.

- [43] L.V. Grigorenko, N.B. Shulgina, M.V. Zhukov, “Three-body vs. dineutron approach to two-neutron radiative capture in ${}^6\text{He}$ ”, *Phys. Lett. B* 807 (2020) 135557.
- [44] L.V. Grigorenko, Yu.L. Parfenova, N.B. Shulgina, M.V. Zhukov, “Asymptotic normalization coefficient method for two-proton radiative capture”, *Physics Letters B* 811 (2020) 135852.
- [45] Yu.L. Parfenova, I.A. Egorova, L.V. Grigorenko, N.B. Shul'gina, J.S. Vaagen, M.V. Zhukov, “From Coulomb excitation cross sections to nonresonant astrophysical rates in three-body systems: The ${}^{17}\text{Ne}$ case”, *Physical Review C* 98 (2018) 034608.
- [46] L.V. Grigorenko, N.B. Shulgina, M.V. Zhukov, “High-precision studies of the soft dipole mode in two-neutron halo nuclei: The ${}^6\text{He}$ case”, *Phys. Rev. C* 102 (2020) 014611.
- [47] Yu. E. Penionzhkevich, Yu. G. Sobolev, V. V. Samarin et al., *Physical Review*, C99 (2019) 014609.
- [48] I. Siváček, Yu.E. Penionzhkevich, Yu.G. Sobolev, S.S. Stukalov, MULTI-2, a 4π spectrometer for total reaction cross section measurements // *Nuclear Instruments and Methods in Physics Research A* Vol. 976 (2020) 164255.
- [49] A. V. Karpov, A. S. Denikin, M. A. Naumenko, A. P. Alekseev, V. A. Rachkov, V.V. Samarin, V. V. Saiko, V. I. Zagrebaev, NRV web knowledge base on low-energy nuclear physics, *Nuclear Instruments and Methods in Physics Research A*, 859 (2017) 112.